Aalto University
School of Chemical
Technology

School of Chemical Technology
Degree Programme of Chemical Technology

Muhammad Saad Qureshi

MEASUREMENT OF ACTIVITY COEFFICIENTS AT INFINITE DILUTION USING THE DILUTOR TECHNIQUE

Master's thesis for the degree of Master of Science in Technology submitted for inspection, Espoo, 17th Sept 2013.

Supervisor **Professor Ville Alopaeus**

Instructor **D.Sc. Petri Uusi-kyyny**
Professor Dominique Richon

Aalto University
School of Chemical
Technology

Aalto University, P.O. BOX 11000, 00076
AALTO
www.aalto.fi

Abstract of master's thesis

Author	Muhammad Saad Qureshi
Title of thesis	Measurement of activity coefficient at infinite dilution using the dilutor technique
Department	Department of Biotechnology and Chemical Technology
Professorship	Chemical Engineering
Code of professorship	KE-42
Thesis supervisor	Professor Ville Alopaeus
Thesis advisor(s) / Thesis examiner(s)	D.Sc. Petri Uusi-kynyy, Prof. Dominique Richon
Date	17.09.2013
Number of pages	76(including Appendixes)
Language	English

Abstract

The goal of this Master's thesis was to design and validate inert gas stripping equipment which would be able to measure activity coefficient at infinite dilution (γ^{∞}) for chemical compounds specially those present in bio-oil.

Activity Coefficient at infinite dilution is an important parameter which is considered when designing rigorous thermal separation processes. The motivation of this research is derived by the absence of γ^{∞} values for various chemical compounds present in bio-oil. In recent future bio based fuels are looked upon as a viable refuge for the growing worldwide energy crisis. Fast pyrolysis of biomass yields bio-oil which has a high potential to be used as an alternative fuel.

Dilutor or inert gas stripping equipment was built as a result of this research. The equipment was validated using Toluene and n-Butanol and γ^{∞} values were also reported for Valeraldehyde for which only very few data points are present in literature. The equipment was tested by changing the flow rate of the inert gas and changing the temperature of the experiment. Effect of hydrophobicity of the chemical compound and effect of vapour pressure of the compounds were also studied.

Keywords IGS, Inert gas stripping, Dilutor, Bio-oil, activity coefficient at infinite dilution, phase equilibrium, VLE

Acknowledgments

First of all I would like to thank Almighty Allah who gave me the strength to fulfill this task properly.

This thesis wouldn't have been possible without the utmost support of my teachers, co-workers and my family.

I would specifically like to thank my Supervisor Prof. Ville Alopaeus who trusted in me and made me a part of his team. His guidance in the research meetings played a very important role in my thesis and eased my work a lot. Secondly my instructor Petri Uusi-Kyyny who constantly guided me throughout the work and helped me achieve the goals of the thesis. I am also grateful to Prof. Dominique Richon for his expert guidance in the equipment building.

I would also like to thanks Piia Haimi and Juha-Pekka Pokki who instructed me on the use of GC and IGS.

Finally I would like to thank my wife Farah Siddiq, my daughter Sana and my whole family in Pakistan who constantly supported me. It would not have been possible for me to complete the thesis without your support.

The thesis was done as a part of the FIDI-pro project.

Muhammad Saad Qureshi
17th September 2013

Nomenclature

Symbols

$\widehat{f_i}$	fugacity for component “i” (Pa)
$\widehat{f_i^l}$	liquid phase fugacity for component ”i” in a mixture (Pa)
$\widehat{f_i^v}$	vapor phase fugacity for component “i” in a mixture (Pa)
A	peak area
a	slope (1/s)
f	fugacity (Pa)
F	flow rate (cm^3/s)
F_{HE}	flow rate of Helium (cm^3/s)
f_i^0	standard state fugacity (Pa)
F_{slv}	solvent gas stream flow rate (cm^3/s)
G	gibbs energy (J)
G_i	gibbs free energy for component “i” (J)
K	proportionality constant
n	number of moles
P	pressure (Pa)
R	universal gas Constant ($Pa\ cm^3\ mol^{-1}\ K^{-1}$)
S	entropy
T	temperature (K)
T_c	critical temperature (K)
T_r	reduced temperature
V	volume (cm^3)
V_g	vapor phase volume (cm^3)
x	liquid mole fraction
y	vapor mole fraction
Z	compressibility factor
ω	acentric factor

Superscripts

i	ideal gas
r	residual property
v	vapor
l	liquid
Sat	saturated
°	standard state

Subscripts

i	component “i”
Solv	solvent
Solu	solute
Out	flow rate out of the dilutor

Abbreviations

DCM	Dichloromethane
DDBST	Dortmund Data bank Software and Separation Technology
DIPPR	Design Institute for Physical Properties
EoS	Equation of State
FID	Flame Ionization Detector
GC	Gas Chromatograph
IGS	Inert Gas Stripping
NIST	National Institute of Standards and Technology
POY	Poynting factor
VLE	Vapor Liquid Equilibrium

Greek

∞	infinite dilution
Φ	fugacity coefficient
γ	activity coefficient

Contents

List of Appendixes

Literature Part

1. Introduction

Phase equilibrium knowledge is the basis for the design of most of separation processes (such as distillation, extraction) involving multiphase equilibria. The data acquired from the phase equilibrium measurements are described by models and interpolated or extrapolated to exploit the state range. There are several ways to determine the properties of the phases in fluid mixtures, though the data in the extreme ranges is scarce (Chapoy, 2004). Activity coefficients at infinite dilution range, particularly important for the thermal separation processes, are not readily available for several systems and efforts have been underway since about three decades now to design equipment that are able to accurately determine this property.

Activity coefficients at infinite dilution are particularly needed when highest efficiency in separation is required. Maximum efforts are required to remove the final traces of the unwanted component from the system (Krummen et al., 2000). Typical separation processes should be very rigorous and highly efficient when it comes to separating the final traces of the component and thus they require higher investments which can be reduced drastically by carefully utilizing the γ^{∞} values. The separation factors (α_{ij}) which are the measure of achievable separation in any thermal separations particularly are highly influenced by the values of activity coefficients γ^{∞}. For example in extractive distillation the addition of selective solvent can significantly change the infinite dilution activity coefficients to obtain the desired separation factors. One of the main benefit of this property is that it can be used to measure the unlike pair interactions in solution without taking into account the dependency of composition. (Eckert and Sherman, 1996)

Infinite dilution activity coefficients find great applicability in many fields ranging from environmental sciences to pharmaceutical industries. Several parameters that are of

great importance to different industries can be derived easily using activity coefficients. For example Henry's constants, partition coefficients, molar excess enthalpies or reliable g^E parameters can be calculated. Richon, 2011 pointed out in his paper how activity coefficients at infinite dilution can be used to determine the solubility of pesticides in water. Solubility of different hydrocarbons in water was measured by different research groups including (Mokraoui et al., 2007). It can be of essential use in waste water treatment industries and oil refineries. Chemical engineering and pharmaceutical industries employ a great use of water for example in the formulation of a new drug. In these cases water-solute interaction parameters are usually needed and they also assist in the design of pollutant control processes. (Chapoy, 2004; Li et al., 1993)

The objective of this research was to design and validate the inert gas stripping equipment that was able to measure γ^{∞} values for a broad range of compounds. The principle compounds of interest focused in this research were bio-oil compounds. Despite of the crucial importance of the bio-based fuels, little attention is paid to the thermodynamic property data acquisition. Fast pyrolysis of biomass results in bio-oil, which contains hundreds of different components in different proportions depending on the pyrolysis conditions and feed stock composition. The thermodynamic data for bio-oil compounds are very important in designing separation technologies including distillation for components segregation. Bio-fuel quality optimization is possible when required separation efficiencies are achieved. In addition to fuel quality, fuel prices are also determined by the quality of fuel. So it is absolutely necessary to acquire enough thermodynamic data to be able to design good feasible bio-fuel plants. We have gathered a database of these bio-oil compounds for which thermodynamic data (esp. VLE and γ^{∞} data) are missing or available only for limited ranges of temperatures.

To validate our apparatus we have used Toluene and n-Butanol as reference compounds in water. The results of γ^{∞} measurements are reported for the range of 298 to 313 K. In addition to the reference system, γ^{∞} values are also reported for Valeraldehyde in water for which γ^{∞} data are mostly missing.

1.1. Phase equilibrium

A phase equilibrium model is needed to express the measured phase equilibrium in a mathematical expression; stringently this model shall be able to incisively predict the properties for phase equilibrium and thermodynamics at all possible combinations of temperatures, pressures and compositions for any component system and possible coexisting phases present. This puts forth a very complex task because all the models have a range of conditions where they work accurately and only in their own ranges they may be used to model different systems reliably. A lot of existing thermodynamic models lie under these three categories.

1. Henry's Law
2. Equations of state models
3. Activity coefficient models

Henry's law is able to predict the phase equilibrium with good accuracy for systems having one or more components in gaseous state and at least one in liquid. The system temperature should be greater than the critical temperatures of both components.

Equations of state models (phi-phi, φ- φ models) are applicable to any combination of temperatures, pressures, compositions and phases. The most popular being "Ideal gas law" is only applicable to gases at ideal conditions.

The activity coefficient models (gamma-phi, γ-φ models) can be applied to systems with temperature not exceeding the critical temperature of any of the systems components.

1.2. Thermodynamic modeling

We consider a closed two phase system having no possibility of the exchange of matter with its surrounding. As equilibrium is established between the phases, both the pressure and the temperature of both phases are equal and there remains no possibility of mass transfer between the phases, i.e. the net mass transfer between the phases is zero. (Raal and Mühlbauer, 1998; Reid et al., 1987; Smith et al., 2005)

The fundamental thermodynamic property relation for homogenous fluid at constant composition gives

$$dG = VdP - SdT \qquad 1\text{-}1$$

The above equation is a definition of the Gibbs energy, a fundamental property of the thermodynamic system, at constant temperature the above equation reduces to

$$dG = VdP$$

Integrating the above equation from a low pressure P* to a higher pressure P at constant temperature yields

$$G^* = G - \int_{P*}^{P} Vdp$$

From the ideal gas law at constant temperature

$$G^* = G - \int_{P*}^{P} \frac{RT}{P} dp$$

As P* approaches zero, the integral approaches to infinity i.e.

$$G^* = G - \infty$$

The difficulty in evaluating the above equation leads to an introduction of the concept of fugacity *f* that has the same dimensions as pressure. It is helpful in describing the real fluid.

$$dG = RTdlnf \quad (constant\ T) \qquad 1\text{-}2$$

A similar equation can be written for ideal gas

$$dG^i = RTdlnP \quad (constant\ T) \qquad 1\text{-}3$$

Difference of the two above equations yields

$$d(G - G^i) = RTdln\frac{f}{P} \quad (constant\ T)$$

The deviation from an ideal state is defined by a property known as residual property; it identifies the magnitude of the deviation of the real from the ideal state. In the equation above the difference in Gibbs energy at the ideal and real states can be termed as G^r, residual Gibbs free energy. The dimensionless ratio of *f/P* is a property of a mixture known as fugacity coefficient φ. The above equation can now be written as

$$dG^r = RTdln\varphi \ (\ constant\ T) \qquad 1\text{-}4$$

The above equation is integrated to give

$$G^r = RTln\varphi + C(T) \quad (\ constant\ T)$$

For an ideal gas the $G^r = 0$ and $f_{ig} = P$. Their ratio φ is 1 which reduces equation 1-4 to

$$G^r = RTln\varphi \quad (\ constant\ T) \qquad 1\text{-}5$$

Equation number 1-2 can be re-written for a component "i" in the system as

$$d\overline{G_\iota} = RTdln\hat{f}_i \quad (\ constant\ T) \qquad 1\text{-}6$$

Where " $\hat{f}_i$ " is the fugacity of component "i" in the solution.

Similarly,

$$\frac{G^r{}_i}{RT} = ln\varphi_i$$

Integrating Equation 1-6 for the change of state from the saturated liquid to saturated vapor both of the states to be at a pressure P^{sat} and temperature T will yield

$$G_i^v - G_i^l = RTln\frac{f_i^v}{f_i^l}$$

Since Gibbs energy change for a constant temperature and constant number of moles is zero, therefore the fugacity of the vapor and the fugacity of the liquid is equal

$$f_i^v = f_i^l = f_i^{sat} = \varphi_i^{sat} P_i^{sat}$$

The relation of fugacity to the pressure at constant temperature can now be expressed as

$$dG_i = V_i dP = RTdlnf_i \ (const\ T) \qquad 1\text{-}7$$

Integrating the above equation from P_i^{sat} to P

$$ln\frac{f_i}{f_i^{sat}} = \frac{1}{RT}\int_{P_i^{sat}}^{P} V_i^l dP = \frac{V_i^l(P-P_i^{sat})}{RT}$$

Substituting the value of $f_i^{sat} = \varphi_i^{sat} P_i^{sat}$

$$f_i = \varphi_i^{sat} P_i^{sat} exp\ [POY] \qquad 1\text{-}8$$

The exponential term in the bracket is called Poynting factor (POY).

1.3. Fugacity Coefficient from Virial EoS

The non-ideality of the vapor phase in a vapor-liquid equilibrium can be predicted by an EoS. The Virial EoS has the basis in statistical mechanics and is expanded by Taylor series. It is able to predict the non-ideality of the vapor phase from low to moderate pressures. A truncated form of the Virial equation is used for calculations whereas the truncation is governed by the temperature and pressure. The initial terms of the equation are

$$Z = 1 + B\left(\frac{P}{RT}\right) + (C - B^2)\left(\frac{P}{RT}\right)^2 + \cdots$$

$$= 1 + \frac{B}{V} + \frac{C}{V^2} + \cdots$$

The coefficients B and C correspond to second and third virial coefficients and Z is the compressibility factor. The Taylor series expansion is truncated to the second term usually because truncation up to second term is usually enough for describing VLE at sub-critical temperatures and pressures up to 1500 kPa. (Perry and Green, 2008)

1.3.1. Estimation of Second Virial coefficient

The basic equation for determining the saturation fugacity coefficient for pure components is

$$ln\varphi_{sat} = \frac{B_{Virial}P_i}{RT} \quad \text{1-9}$$

The Second virial coefficient (B) was calculated using Tsonopoulos, 1974 correlation which is

$$B_{virial} = \left(\frac{RT_c}{P_c}\right)\left[B^{(0)} + \omega B^{(1)}\right] \quad \text{1-10}$$

Where,

$$B^{(0)} = 0.1445 - \frac{0.33}{T_r} - \frac{0.1385}{T_r^2} - \frac{0.0121}{T_r^3} - \frac{0.000607}{T_r^8}$$

$$B^{(0)} = 0.0637 + \frac{0.331}{T_r^2} - \frac{0.423}{T_r^3} - \frac{0.008}{T_r^8}$$

Where $T_r = T/T_c$.

This correlation is widely used for the estimation of second virial coefficient and provides good results for both polar and non-polar substances.

1.4. Activity Coefficient

It is sometimes useful to represent the vapor and liquid phase fugacities according to the functions they are dependent on. As the vapor phase composition is usually expressed by the mole fraction y, thus to relate the vapor phase fugacity f_i^v to the mole fraction, temperature and pressure, fugacity coefficient φ_i for vapor phase can be used

$$\varphi_i{}^v = \frac{f_i^v}{y_i P} \qquad 1\text{-}11$$

In order to characterize the liquid-phase non ideality (in phase equilibrium) a new term i.e. the "activity coefficient" is used and it has a similar definition as the vapor phase fugacity, it can be written for the mole fraction of liquid x_i as

$$\gamma_i = \frac{f_i^l}{x_i f_i^\circ} \equiv \frac{a_i}{x_i} \qquad 1\text{-}12$$

Where a_i is the activity coefficient of component i and f_i° is the standard state fugacity of the component "i" at the system temperature.

The criterion for the equilibrium as stated earlier dictates that both the vapor and the liquid fugacities must be equal i.e.

$$\hat{f}_i^l = \hat{f}_i^v$$

Comparing equations 1-11 and 1-12 and solving for the vapor mole fraction gives

$$y_i = \frac{x_i \gamma_i f_i^\circ}{\varphi_i{}^v P}$$

The value of f_i° can be substituted for the standard state fugacity.

$$y_i = \frac{x_i \gamma_i \varphi_i^{sat} P_i^{sat} exp\,[POY]}{\varphi_i{}^v P} \qquad 1\text{-}13$$

$$y_i = \frac{x_i \gamma_i P_i^{sat}}{\varphi_i P}$$

Where,

$$\varphi_i = \frac{\hat{\varphi}_i}{\varphi_i^{sat}} exp[-POY] \qquad 1\text{-}14$$

The above equation is a general correlation representing vapor and liquid mole fractions assuming the liquid is incompressible. The exponential term in the parenthesis is known as Poynting correction factor which corrects for the pressure effect on the liquid phase fugacity because the pressure p can strongly deviate from vapor pressure at system

temperature. The effect of the pressure is not considerable on the liquid phase fugacity if the temperature is well below critical, and if the pressure difference is not too large the Poynting factor can be approximated to 1. In cases where pressure p is well above the vapor pressure, the product of saturation fugacity coefficient and Poynting factor can easily exceed unity (Reid et al., 1987).

1.5. Methods and their limitations

Experimental methods utilized to determine the infinite dilution activity coefficient are reviewed very comprehensively by Kojima et al. (Kojima et al., 1997). They can be classified as

1. Direct methods
    a) Gas liquid chromatography (GLC)
    b) Head-Space Chromatography
    c) Gas Stripping
    d) Differential ebulliometry
    e) Liquid-liquid chromatography
    f) Differential static method
    g) Dew point method
    h) Inverse Solubility

2. Indirect Methods
    a. VLE and LLE interpolations and extrapolations
    b. Gas-liquid partition coefficient data

1.5.1. Gas-liquid chromatography

The oldest and still popular method for the direct measurement is Gas-liquid chromatography which dates back to 1952. The technique was used to determine the elution time of the solute in the presence of very small amount of solvent. This can be utilized to measure the Henry's constants also. It was first proposed by James and Martin, 1952 and found a great use in measuring the activity coefficients where the solute is volatile and the solvent is non-volatile; however later in the 1980s modified techniques were developed to use the high volatile solvent and low volatile solute. In their study Thomas et al., 1982) examined 34 different solvents covering wide range of polarizability. They addressed the problems of using Chromatographic method with high volatility solvents. One of the problems was the reduction in solvent composition due to gas-phase expansion which according to them could be eradicated by introducing the same amount of solute at the beginning and the end of the run and by the operation at low pressure drop. They were however not able to generate very good γ^{∞} values and especially those having values above 100. It was in 1972 the non-steady state GLC technique was introduced (Belfer, 1972). It did not gain much popularity for over a decade. As described by the same author in his later research (Belfer and Locke, 1984) the idea was to have both the carrier gas and the solvent mobile. The open tubular column was not loaded with the solvent as in conventional GC but it was injected and adsorbed on the walls of the capillary having silica. When the equilibrium was reached, the elution of the solvent linearly decreased and the solute retention time decreased. This retention time was used to measure γ^{∞} values. Although some of the common problems faced in conventional methods were rectified, it cannot be precisely said that the non-steady state GLC was a better choice because the technique only worked better with low volatility solvent and was not applicable to mixed solvent systems.

1.5.2. Head-Space analysis

Another development during the same time was the head-Space GLC which was able to accurately measure the vapor phase composition. An improved version of this technique (Li and Carr, 1993) has been presented.

Figure 1 Modern Headspace Chromatography, courtesy Perkin Elmer

The basic idea exploited was the change in concentration of vapor in equilibrium with dilute solution upon the addition of known solvent. This can be used in calculating the partition coefficient of the solute in gas and solvent which can be further used to calculate the γ^{∞} values. Head-Space can be broadly classified as dynamic or static. A more conventional static method was based on the idea that vapor in equilibrium with the dilute solution can be drawn from a sealed vial and can be fed to a GC. Sampling could be pressurized or through a syringe, whereas in dynamic head-space analysis the gas was collected on a sorbent and analyzed (Snow and Slack, 2002). In their review, (Kojima et al., 1997) these authors pointed out that headspace GLC had shown promising results with mixed solvents and can be greatly exploited for the measurement of series of solute, although the major drawback are the calibration requirement of detector. The volatility of the solute must be large enough to be analyzed for the concentration.

1.5.3. Differential ebulliometry

Differential ebulliometry commonly known as the boiling point method also emerged as a promising technique of studying the vapor liquid equilibrium. The method was based on the idea of measuring the difference in boiling point temperatures of a dilute solution in a measuring ebulliometer and the pure solvent in a reference ebulliometer as a function of the composition under constant pressure. Eckert et al. (1981) in their research article emphasized that the most convenient methods are 1) Gravimetric determination of composition. 2) Dynamic vapor-liquid equilibrium to quickly obtain the measurement.

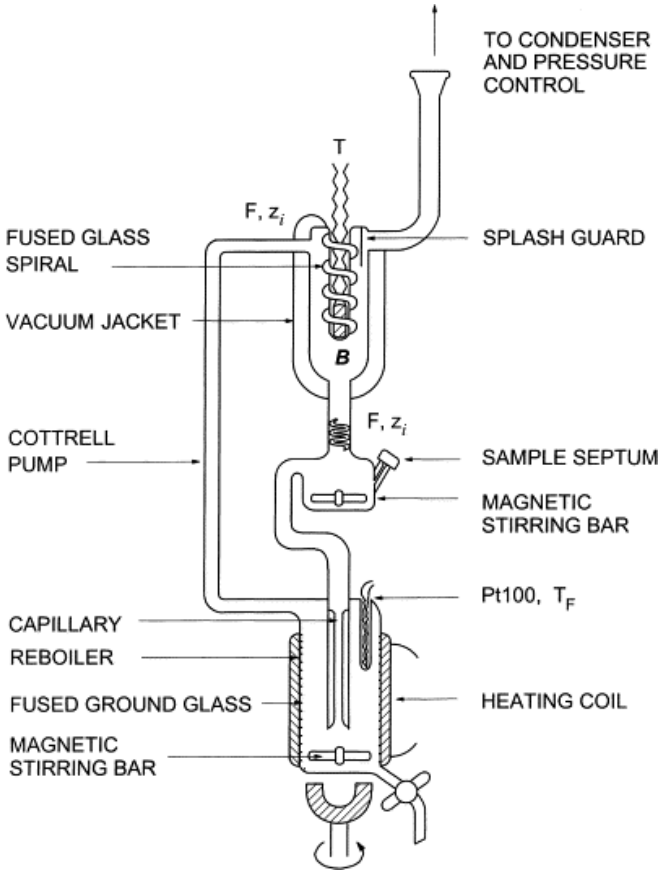

Figure 2 Schematic Differential Ebulliometer (Raal et al., 2001)

An improvement in design of differential ebulliometer was made by the same research group next year. Thomas et al., 1982 analyzed about 147 systems and found the results to be well consistent. To have better results with the ebulliometry it is required to have systems that have their boiling point temperatures close to each other. Pointed out by many researchers, ebulliometry is best suitable with systems involving water. The accuracy is objectionable when the boiling point difference of the components is high.

1.5.4. Head-Space-SPME

A new technique for γ^{∞} determination was developed in 2012 (Furtado and Coelho, 2012). It implies the use of SPME (Solid Phase Micro Extraction) in conjunction with Head-Space. The solute particles from the Head-Space of the solution containing vial are absorbed on the polymeric coating on the extractor fiber rod. This coating containing the solute is further analyzed through the Head-Space. The quantification of the analyte determines the activity coefficient at infinite dilution.

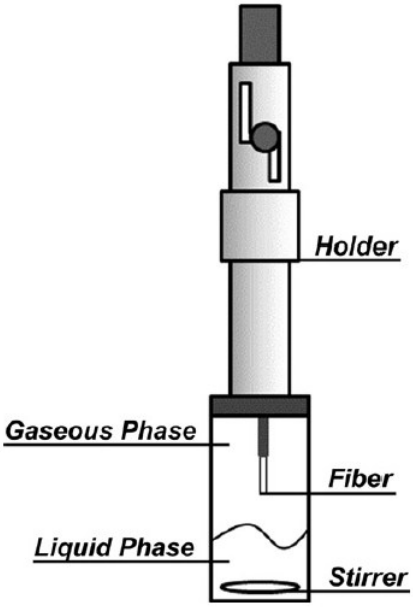

Figure 3 HS-SPME schematic (Furtado and Coelho, 2012)

The amount of solute absorbed on the polymeric coating is a property of the type of polymer coated on the rod, temperature, pressure and physical characteristics of coating. The amount of analyte extracted by the coating is proportional to the concentration of the analyte in the solvent provided the equilibrium is attained. The length of the exposure to the solute may vary from 2 minutes to 1.5 h depending on the nature of the solute. The activity and partition coefficients are reported for different hydrocarbons in Furfural at different temperatures and the results are very close to the literature values (Furtado and Coelho, 2012) showing the precision of the technique. The technique was also validated with extensive replication on finding dimensionless Henry's law constants for four Volatile Organic Compounds (Böhme et al., 2008). The results in this research were compared with results from independent Inert Gas Stripping technique in a complete different environment and the results agree with in 5% deviation. They pointed out that conditioning of the SPME fibers before sampling is necessary to avoid any thermal difference and that prolongation of thermodesorption of the fiber content leaves behind nothing on the fibers.

The advantages of this technique include simplicity of analysis, low cost, reusability of the fiber rod, absence of solvent in the sample, high sensitivity and determination limit and range of compounds that can be analyzed. However few limitations of the equipment as stated in the same article are the swelling rate of the fiber which may lead to the removal of polymeric material from the fiber and affinity of the solvent towards the fiber which must also be small as possible. The polymer coating is also fragile and must be carefully handled.

1.5.5. Inert Gas Stripping

The idea of gas stripping to calculate the γ^{∞} values was generated with the work of (Fowlis and Scott, 1963). He used the gas stripping technique to calibrate the Chromatographic detectors for their linearity in the concentration range. In the same year Burnett et al. (1963) also used the same dilution technique for the determination of

partition coefficients at infinite dilution; the results are in good agreement with other available data.

The basis of the idea was the measurement of the variation of vapor phase composition with the help of an inert gas, stripping the solute from the solution. The vapor phase analyzed by gas chromatography had to be in equilibrium with the solution. Leroi et al. (1977) exploited this idea and derived a relation between the variation of vapor phase composition and infinite dilute activity coefficient. This was perhaps the first attempt to infer γ^{∞} values from the gas stripping technique. Several VLE systems that he analyzed are in good agreement with the VLE extrapolation results; however some deviations are observed when the results are compared to the retention time method. The experiments were conducted in a special dilutor cell which was in fact first of its kind. The only limitation at this stage was the viscosity of the system. Dilutor cell only worked with systems having viscosity less than 20 cP. Other limitation is that the solute had to be volatile enough to be used for the law of elution.

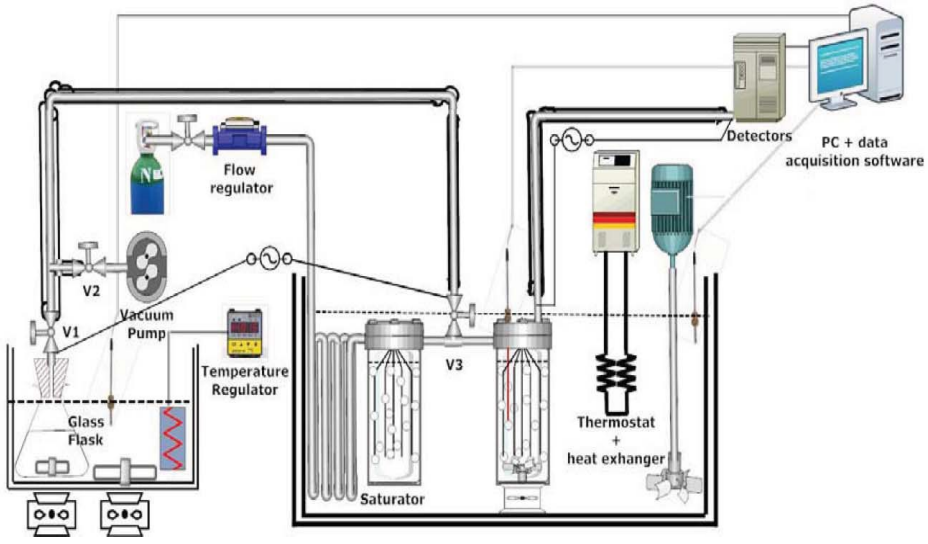

Figure 4 Inert Gas Stripping with saturator cell and capillaries (Richon, 2011)

Richon et al., 1980 came up with a new design of the dilutor cell. The design was based on more careful mass transfer calculation. Thin capillaries were used to introduce the solute gas into the dilutor cell, which improved the mass transfer. Infinite dilution activity coefficients for linear and branched alkanes were calculated in n-hexadecane solvent and results that he got are in good agreement with the available experimental

values. However there are still some shortcomings of the design and the major ones reported are 1) longer elution times for higher chain alkanes. 2) Poor determination of equilibrium because of the design of the cell. 3) Inability to use the cell to measure high values of the Henry's Constants. The cell was only able to work low viscosity systems, thus in order to overcome these limitations a new dilutor was designed which had a completely different gas liquid contact system and this cell has the capability to work on systems with high viscosity even up to 1000 cP (Richon et al., 1985). It was pointed out in his research paper that glass fritted disk do not produce consistent small size bubble and there is also a possibility of coalescence. However Li et al. (1993) pointed out that glass fritted disk having pore diameter of about 4 μm are able to produce the bubble size of less than 1 mm and also that no coalescence was observed. In their research they calculated the γ^{∞} values of non-electrolytes in water system and found the measurements to be in good agreement with values calculated from inverse solubility method. The cell he designed was based on the model of Richon et al. (1985) however had the following limitation. The cell was not able to work for system having low gas to vapor partition coefficient (K) because mass transfer with insoluble solutes was poor. The value of the partition coefficient determines the validity of the operating range of the equipment. This value is a function of bubble size, mass transfer coefficient in solvent and the velocity of the bubbles inside the solution.

Gas stripping technique was initially confined to vapor phase analyses. However later attempts were made to analyze the liquid phase instead of vapor and the results were in good comparison with vapor phase measurements (Wobst et al., 1992). The main advantage of this method is its ability to measure the γ^{∞} values for systems having low volatility. The method is also suitable to highly dilute and volatile substances in mixtures that did not precisely follow Raoult's law which assumes that the partial vapor pressure of the component in the gaseous mixture above the solution is a product of the vapor pressure of that pure component and its mole fraction in the mixture i.e. $P_i = P_i^{sat} x_i$. Sancho et al., 1997 measured the activity coefficients for apple juice aroma compounds at infinite dilution in water based systems. The results obtained were not very satisfactory in comparison to results calculated from UNIFAC contribution method The UNIFAC results were more closer to the literature values. However predictive methods like UNIFAC cannot be the basis of reliable comparison because they can

predict very absurd values. A -80 to 118% deviation was observed. Solvent concentration in the dilutor should remain constant throughout the experiment; this is possible by the upstream addition of a saturation cell to the dilutor.

Krummen et al., 2000 explains the advantage of using a presaturator cell. Both the saturator cell and the dilutor were designed by Prof. D. Richon from Ecole Nationale Supérieure des Mines de Paris, France. Activity coefficient values, γ^{∞}, of different straight chain and aromatic hydrocarbons in ionic liquids were measured in the same equipment (Krummen et al., 2002). Aliphatic hydrocarbons show strong deviation from Raoult's law in Ionic Liquids. This phenomenon can be exploited in extractive distillation or extraction. No significant improvement in inert-gas stripping (IGS) technique was reported until a recent article by Prof. D. Richon (Richon, 2011), where he described some improvement from the previous design. He pointed out that the new design was able to rectify measurement errors caused by the adsorption of solute on the walls of the transfer line or on the sampling valves and that this design was able to produce results far quicker than any other previous dilutor versions.

Although recent developments in the IGS technique have opened doors for wider research opportunities in systems involving organic compounds, aqueous solutions and ionic liquids, there are still some improvements deemed in the design to cope up with the issues of lower volatility systems.

1.6. Activity Coefficient at infinite dilution

The activity coefficients at infinite dilution can be determined by assuming equilibrium between the gas and the liquid phase according to equation 1-13 (Gmehling et al., 2012; Krummen et al., 2000)

$$y_i = \frac{x_i \gamma_i \varphi_i^{sat} P_i^{sat} POY_i}{\varphi_i{}^{v} P}$$

A similar equation representing the same phenomenon can be written for the solvent

$$y_{solv} = \frac{x_{solv}\gamma_{solv}\varphi_{solv}^{sat}P_{solv}^{sat}POY_{solv}}{\varphi_{solv}{}^{v}P} \qquad 1\text{-}15$$

since the solute has to be in infinitely dilute range (about $x_i < 10^{-3}$) and as described earlier, depending on pressure difference the Poynting factor can be approximated to 1. In dilution technique the carrier gas is chosen as inert and the solubility of this gas in the liquid phase can be neglected (Krummen et al., 2000). The assumptions made for the mathematical expressions are,

(1) $\gamma_i = \gamma_i^{\infty}$ (infinitely dilute)
(2) $\gamma_{solv} = 1$ (pure solvent)
(3) $POY_i = 1$ (pressure difference)

Since the carrier gas is inert, the vapor phase fugacity coefficient $\varphi_i{}^{v}$ can be approximated to one and also for the solvent

$$\frac{\varphi_{solv}^{s}POY_{solv}}{\varphi_{solv}^{v}} \approx 1$$

The simplifications above reduces 1-13 to

$$y_i = \frac{x_i\gamma_i^{\infty}\varphi_i^{sat}P_i^{sat}}{P} \qquad 1\text{-}16$$

Similarly the equation can be written for the solvent i.e.

$$y_{solv} = \frac{P_{solv}^{sat}}{P} \qquad 1\text{-}17$$

In a dilutor equipment where two cells are used for determination of activity coefficient as in Fig 5.

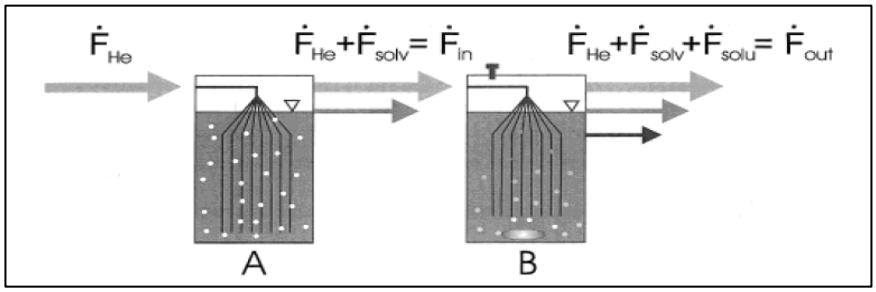

Figure 5 Schematic flow of the dilutor cell (Krummen et al., 2000)

Cell A is used as a saturator and Cell B is the dilutor. The details of the techniques are in section 6. The stream entering the dilutor cell is composed of the carrier gas (Helium in this case) and the Solvent gas stream i.e.

$$F_{in} = F_{He} + F_{solv} \quad \text{1-18}$$

The solvent flow is a function of the vapor pressure of the solvent and the carrier gas flow i.e. $F_{slv} = F_{He} y_{solv}$.

Substituting eq. 1-17 in 1-18 yields

$$F_{in} = F_{He}(1 + \frac{P_{solv}^{sat}}{P})$$

As the experiment proceeds the amount of the solute in the dilutor cell decreases, an expression describing the elution of the solute from the dilutor cell can be written as

$$F_{solu} = -\frac{RT}{P}\frac{dn_{solu}}{dt}$$

Basic material balance implies

$$F_{out} = F_{in} - \frac{RT}{P}\frac{dn_{solu}}{dt} \quad \text{1-19}$$

The rate of decrease of the solute in the dilution cell can be written in the form of the mole fraction eluted and the flow out of the cell.

$$\frac{dn_{solu}}{dt} = -y_{solu}\frac{PF_{out}}{RT} \quad \text{1-20}$$

The saturator cell ensures that the carrier gas is saturated with the solvent and that during the experiment there is no change in the composition of the solvent in the measurement cell.

$$\frac{dn_{solv}}{dt} = 0$$

Equation 1.20 can be substituted in equation 1.19 giving

$$F_{out} = \frac{F_{in}}{1-y_{solu}} \quad 1\text{-}21$$

Equation 1.16 can be substituted in equation 1.21

$$F_{out} = \frac{F_{in}}{1-\frac{x_i\gamma_i^{\infty}\varphi_i^{sat}P_i^{sat}}{P}} \quad 1\text{-}22$$

Equation 1.22 and equation 1.16 can be substituted in equation 1.18 yielding

$$\frac{dn_{solu}}{dt} = -x_i\gamma_i^{\infty}\varphi_i^{sat}P_i^{sat}\frac{F_{in}}{\left(1-\frac{x_i\gamma_i^{\infty}\varphi_i^{sat}P_i^{sat}}{P}\right)RT} \quad 1\text{-}23$$

The total number of moles of solute in the measurement cell will be the sum of their moles in the liquid and their number of moles in the gas phase i.e.

$$n_{solu} = n_{solu}^{v} + n_{solu}^{l} \quad 1\text{-}24$$

Where the number of the moles of the solute in the liquid phase can be written as

$$n_{solu}^{l} = x_{solu}n_{solv} \quad 1\text{-}25$$

and content of the solute in the gas phase can be written as

$$n_{solu}^{v} = y_{solu}\frac{PV_g}{RT} \quad 1\text{-}26$$

Substituting 1.26 and 1.16in equation 1.24

$$x_{solu} = \frac{n_{solu}}{n_{solv}\left(1+\frac{\gamma_i^{\infty}\varphi_i^{sat}P_i^{sat}V_g}{n_{solv}RT}\right)} \quad 1\text{-}27$$

The mole fraction of the solute can be substituted in eq.1.23

$$\frac{dn_{solu}}{dt} = \frac{n_{solu}}{n_{solv}\left(1+\frac{\gamma_i^{\infty}\varphi_i^{sat}P_i^{sat}V_g}{n_{solv}RT}\right)}\gamma_i^{\infty}\varphi_i^{sat}P_i^{sat}\underbrace{\frac{1}{\left(1-\frac{\gamma_i^{\infty}\varphi_i^{sat}P_i^{sat}n_{solu}}{Pn_{solv}\left(1+\frac{\gamma_i^{\infty}\varphi_i^{sat}P_i^{sat}V_g}{n_{solv}RT}\right)}\right)}}_{\text{Corrective term}}\frac{F_{in}}{RT} \quad 1\text{-}28$$

The solute concentration in the gas stream reduces as the solute is stripped out but this reduction can be neglected if compared to the inert gas stream and the value of the corrective term can be approximated to unity. The integration of the above term therefore does not need to take the corrective term into account, however in the cases where the solute gas stream reduction is considerable compared to inert gas stream then this term would be included. Eq 1-28 reduces to 1-29 when the corrective term is neglected

$$ln\left(\frac{n_{solu}}{n_o}\right) = -\frac{\gamma_i^{\infty}\varphi_i^{sat}P_i^{sat}}{n_{solv}\left(1+\frac{\gamma_i^{\infty}\varphi_i^{sat}P_i^{sat}V_g}{n_{solv}RT}\right)}\frac{F_{in}}{RT}t \qquad 1\text{-}29$$

If partial pressure of the solute is proportional to the amount of solute injected in GC and if there is complete heat tracing for the lines leading to the detector in GC, i.e. making sure that there is no chance of condensation in the line then the following relation can be applied

$$A_{solu} = ky_{solu}P \qquad 1\text{-}30$$

Where, A represents the area of the peak generated by the GC for the solute and "k" is the proportionality constant. $y_{solu}P$ in the above equation can be substituted by 1.14 and 1.25 giving

$$A_{solu} = k\left[\frac{\gamma_i^{\infty}\varphi_i^{sat}P_i^{sat}}{n_{solv}\left(1+\frac{\gamma_i^{\infty}\varphi_i^{sat}P_i^{sat}V_g}{n_{solv}RT}\right)}\right]n_{solu} \qquad 1\text{-}31$$

If the value of n_{solu} from the above equation is inserted in 1.29 it yields

$$\frac{ln\left(\frac{A_{solu}}{A_o}\right)}{t} = -\frac{\gamma_i^{\infty}\varphi_i^{sat}P_i^{sat}}{n_{solv}\left(1+\frac{\gamma_i^{\infty}\varphi_i^{sat}P_i^{sat}V_g}{n_{solv}RT}\right)}\frac{F_{in}}{RT}$$

Solving for γ_i^{∞} and substituting $\frac{ln\left(\frac{A_{solu}}{A_o}\right)}{t}$ as "a", slope. We get

$$\gamma_i^{\infty} = -\frac{n_{solv}RT}{\varphi_i^{sat}P_i^{sat}\left(\frac{F_{in}}{a}+V_g\right)} \qquad 1\text{-}32$$

Equation 1-32 is used for determining the infinite dilution activity coefficient of the solute in the solvent.

Experimental Part

2. Compounds of interest

Increased usage of the fossil fuels with the growing world population and economic progress necessitates the urge to explore alternative energy resources. In recent years there has been a lot of research on bio-based compounds as a possible refuge for the growing energy crisis. Biorefineries will play an important role in the future sustainable bioeconomy. Despite of the crucial importance of Biorefineries in the near future only little data is available on the thermodynamic properties. Biomass which is the principal feedstock of the bio refineries can be converted to various value added products through different chemical routes. Fast pyrolysis of the Biomass yields in Bio-oil which has a potential to be used both as heavy and light fuel oil (Oasmaa et al., 2011).

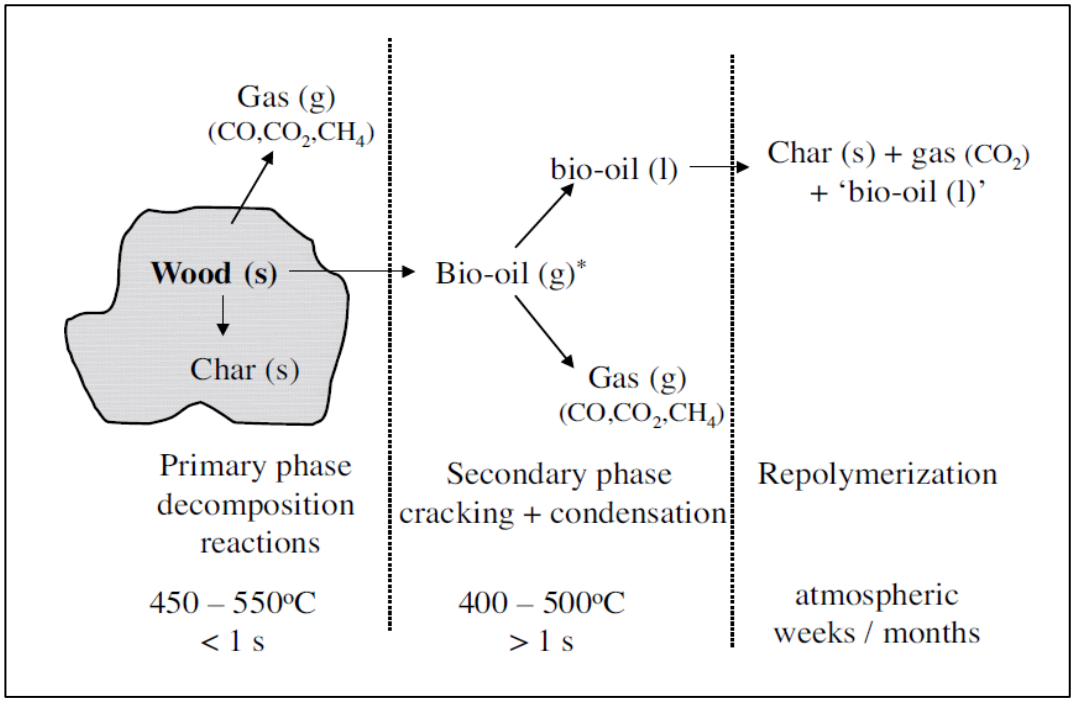

Figure 6 Reaction paths for wood Pyrolysis (Brown, 2011)

Extensive research is done on the chemical and physical properties of bio-oil however little or no data is published on the thermodynamic properties stating phase equilibria of bio-oil components. In this work, phase equilibrium studies of the bio-oil components are carried out.

The composition of bio-oil depends on type of biomass and the production conditions: high temperature pyrolysis yields small proportion of bio oil and more condensable gases while slower pyrolysis leads to larger amount of coke (Li and Paricaud, 2012). Bio-oil can be characterized in to water soluble and water insoluble fractions. Chemical characterization of the Bio-oil is given in the figure 7.

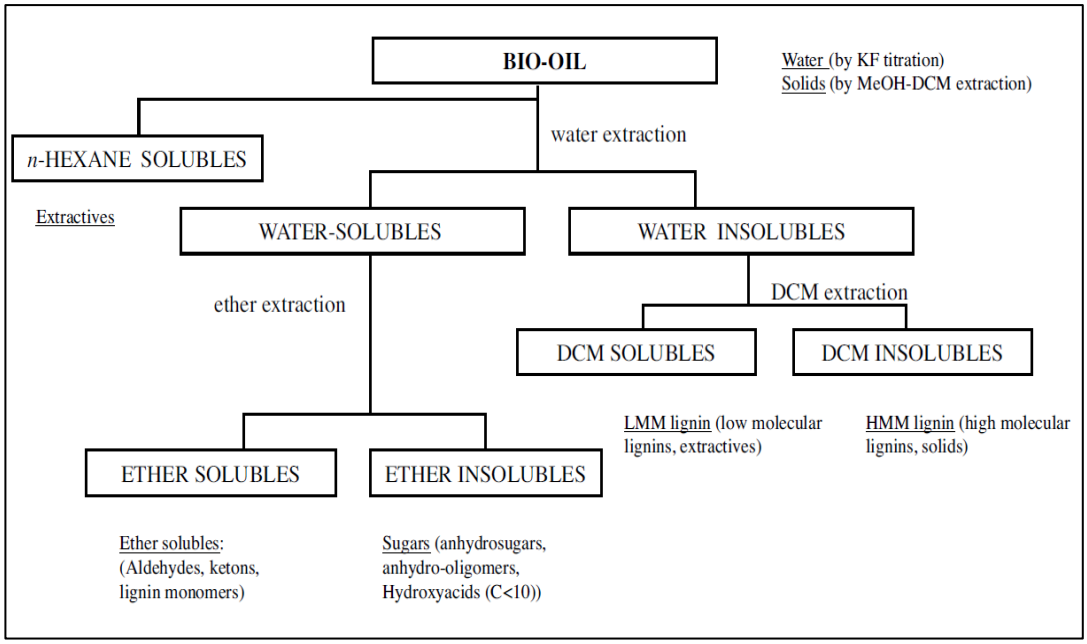

Figure 7 Chemical Characterization of Bio-oil (Oasmaa et al., 2003)

2.1. Properties of Bio-oil

The property of Bio-oil depends largely on the pyrolysis reaction conditions and feed stock composition. The pyrolysis liquid obtained from forestry residue separates into two phases on condensation, the top liquid (10-20 wt %) is hydrophobic and the lower bottom liquid (80-90 wt %) is polar in nature. The polarity in the bottom phase is due to

the presence of oxygenated compounds. The color of bio-oil can vary from dark brown to black depending on the char present in the liquid. The density of the liquid is about 1200 kg/m^3 and the viscosity varies from 25 to 1000 cP, depending on the water content (Brown, 2011), Owing to the presence of carboxylic acids (acetic and formic acid) as a result of degradation in the bio mass constituents, the pH of bio-oil can vary from 2 to 4.

Table 1 Elemental composition and properties for wood derived bio-oil (Brown, 2011)

Physical Properties		***Pyrolysis Conditions***	
		temperature (K)	750-825
Water content (wt %)	15-30	gas residence time (s)	0.5-2
pH	2.8-3.8	particle size (μm)	200-2000
density (kg/m^3)	1050-1250	Moisture (wt %)	2-12
		Cellulose (wt %)	45-55
		Ash (wt %)	0.5-3
Elemental Analysis (wt% moisture free)			
C	55-65	***Yields (wt %)***	
H	5-7	organic liquid	60-75
S	0.00-0.05	water	10-15
N	0.1-0.4	char	10-15
O	Balance	gas	10-20
Ash	0.01-0.30		
Higher Heating Value (10^6 J/kg)	16-19		
Viscosity (315K, cP)	25-1000		
ASTM vacuum distillation (wt %)		***Solubility (wt %)***	
430 K	~10	hexane	~1
466 K	~20	toluene	15-20
492 K	~40	acetone	>95
distillate	~50	acetic acid	>95

The oil is corrosive and must be kept in acid proof containers. The water content of the bio oil can limit its applications in some cases because it reduces the higher heating value of the oil to 19 x 10^6 J/kg which is significantly less than the conventional fossil fuel. This problem can however be reduced by the extensive drying of the bio mass which will significantly reduce the water content in the bio oil. Thermal separation of water may not be suitable for bio oil because at higher temperatures bio oil tends to polymerize. The properties of the bio oil changes with time as well. This includes the viscosity increase, formation of CO_2 or the increase in the water content (mainly because of the phase split over time). Various analytical techniques have been used in

the recent years to classify the chemical composition of the bio oil but some techniques including GC have a limited use for its classification. One of the major reasons for the limitation is the presence of the non-volatile components in bio oil. The techniques themselves pose limitation for the chemical classification sometimes such as their destructive effect on the analyte. To cope up with these challenging researches, new techniques are ongoing and potentially viable and non-destructive techniques are used such as solvent fractionation. Chemical classification of Pine oil (Brown, 2011) is presented in Table 2. The method used for this classification includes the use of solvent extraction in conjunction with GCMS (Gas chromatography mass selective) detection.

Table 2 Chemical Composition of reference Pine oil (Brown, 2011)

Chemical Composition of reference Pine Oil (wt %)						
	Wet	**Dry**	**C**	**H**	**N**	**O**
Water	23.9	0				
Acids	4.3	5.6	40	6.7	0	53.3
Formic acid		1.5				
Acetic acid		3.4				
Propionic acid		0.2				
Glycolic acid		0.6				
Alcohols	2.23	2.9	60	13.3	0	26.7
Ethylene glycol		0.3				
Isopropanol		2.6				
Aldehydes and ketones	15.41	20.3	59.9	6.5	0.1	33.5
Nonaromatic aldehydes		9.72				
Aromatic aldehydes		0.009				
Nonaromatic ketones		5.36				
Furans		3.37				
Pyrans		1.1				
Sugars	34.44	45.3	44.1	6.6	0.1	25.2
1,5-Anhydro-b-D-arabino-furanose,		0.27				
Anhydro-b-D-glucopyranose (levoglucosan)		4.01				
1,4:3,6-Dianhydro-a-D-glucanpyranose,		0.17				
LMM lignin	13.44	17.7	68	6.7	0.1	25.2
Catechols		0.06				
Lignin-derived v		0.09				
Guaiacols (methoxyphenols)		3.82				
HMM lignin	1.95	2.6	63.5	5.9	0.3	30.3
Extractives	4.35	5.7	75.4	9	0.2	15.4

2.2. Validation

To validate our results from the dilutor, Toluene and 1-Butanol in water were used as reference systems. Initial runs were not successful but after some modifications with the design of the dilutor (see fig 8.) we managed to get the results of activity coefficients comparable to the literature value. As already described the aim was to design equipment which is able to measure the activity coefficient values at infinite dilution for the components present in bio-oils. A vast literature search was carried out thanks to DDBST and NIST; the list was gathered for the bio-oil components for which the VLE was unknown (see Appendix F.) Although the measurements will be carried out for other components in the continuation of this work, in this study only two new components are considered for which the VLE data are either limited or not available. These are Valeraldehyde and n-Hexanoic acid. The reason behind their selection for initial runs was that sufficient γ^{∞} values for small chain acids and aldehydes are available in literature and these selected compounds owing to the fact that they belong to the same hydrocarbon family were expected to exhibit a similar behavior.

3. Equipment Building

3.1. Design and construction

There are three major sections of the equipment. 1. Gas supply. 2. GC with dilutor assembly. 3. Signal converter and computer. The dilutor assembly as shown in Fig. 8 is fitted inside the GC oven. This assembly mainly consists of two glass cells (see Fig. 9) of same or different volumes which are attached to a stainless steel lid with the help of an adjustable iron clip. The lids were initially made of Teflon but they failed to prevent leakages because frequent tightening of screws in Teflon cause thread slips so they were replaced by stainless steel. Inert gas (Helium) flow via an electronic flow meter (MC-10SCCM-D from ALICAT scientific) and is directed to the Saturator cell in Copper tubing which is coiled in multiple turns and stays inside the GC oven. The coiling of tube is necessary to provide enough residence time for gas to attain temperature of the GC. This copper tubing is attached to the other tube with Swagelok fitting as indicated in the figure 10. The tube is brazed to the lid and has seven stainless steel capillaries (0.2 mm internal diameter and 0.4 mm outer diameter) also brazed on the rear end. This setup makes it possible to bubble the inert gas inside the saturator cell. These thin capillaries make sure that the bubbles are of same size and relatively small compared to the glass fritted disk. The size of bubbles are important to consider because the smaller the bubbles the greater the surface area and better the mass transfer. It is important to use the saturator cell in conjunction of the dilutor cell because it keeps the mass of the solvent inside the dilutor constant. It is also possible to use cells of different volumes for the saturator however we have used the cell that has a volume of 19.3 cm^3. The cell volume used in the calculations had the capillary and magnetic stirrer volume excluded. A silicon ring in between the attachments of the lid and the glass cell prevents any leakages. Saturated gas travels from the first cell to the dilutor cell through a tube which also has these capillaries on the other end. The Dilutor cell has exactly the same setup but the stripping gas is now directed to the FID (Flame Ionization detector) where it is analyzed. The tube delivering the gas from the dilutor to the detector, about 10 cm long, is electrically traced by a 50 W heating coil to avoid any condensation. Solutions inside

the two cells are kept stirred with the help of the magnetic stirrer and it is possible to vary the stirring speed.

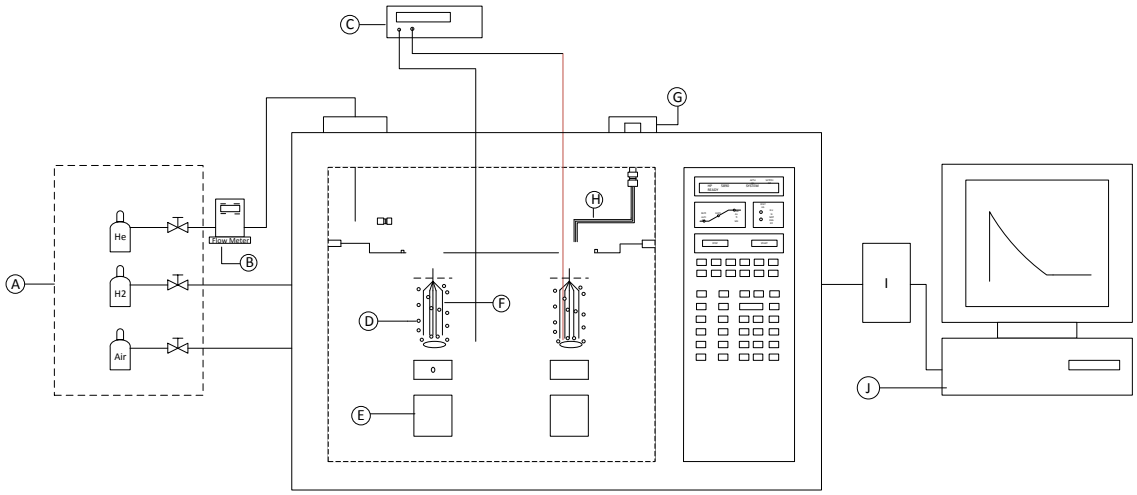

Figure 8 Dilutor Setup schematic

A- Gas supply, B- Mass flow controller, C- Temperature recorder, D- Glass cell, E- Magnetic Stirrer, F- Capillaries, G- FID detector, H- Electrically traced line, I- Signal converter, J- Computer.

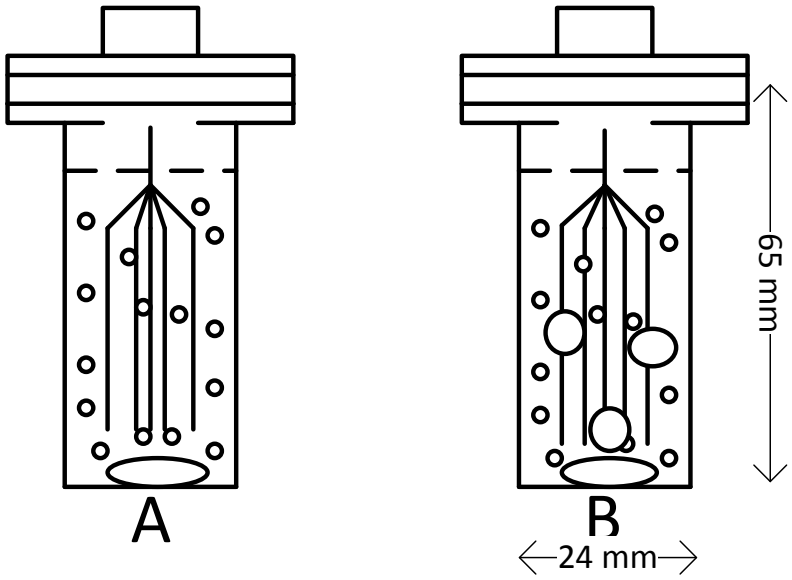

Figure 9 A. slow stirring B. fast stirring

The stirring also increases the retention time of the bubbles. However, care must be taken that the stirring speed is not so high that it coalesces the tiny bubbles to form a bigger size bubble (see fig 9.) which disturbs the equilibrium in the vapor phase. The temperature of the solution is recorded with the Platinum 100 RTD (resistance temperature detector) dipped inside the cell. An extra RTD is also available to measure the room temperature or the temperature of the GC oven, however it is possible to observe the temperature of the oven on the interface of the GC but it is not real time and with present setup it cannot be recorded. The temperature signal is read off the temperature indicator (ASL-F200 precision Thermometer). The FID signal is acquired from the network interface card and is converted to volt signal scaled from 0 to 1 in a 4 channel Universal Analog Input module (National Instruments). The converted signal is recorded in a text file which is created by Lab View software.

3.2. Operation

A typical experiment starts by weighing a premixed solution in the dilutor cell (solution preparation is discussed in detail later). The saturator cell is filled by the solvent (distilled water in this case) half way up; the depth must be enough to immerse all the capillaries well inside the solvent. The longer the capillaries, the longer the path will be for the bubbles and greater the mass transfer will be to achieve equilibrium, however the optimum length of the capillaries are dependent on the size of the bubble it will produce and the dimensions of the cell. A detailed mass transfer study is done by Prof. Richon (Richon et al., 1980). The mass transfer of the solute gas in a solvent is governed by two individual steps. 1. Mass transfer in the liquid phase. 2. Diffusion in the gas phase. Experimental studies involving different solvents and solutes with different bubble diameter and height of liquid were carried out in his study and he concluded that the bubble diameter must be as small as possible and the path length is then the function of the bubble diameter. For detailed mass transfer study in our case see appendix E.

The dimensions of the cell in our work can be seen from fig 9. The dilutor cell is clipped to the lid such that there is no leakage possibility. The magnetic stirrer is set to a speed around 1000 rpm or less; the speed must be so that it does not project the liquid as an entrainment to the gas exit.

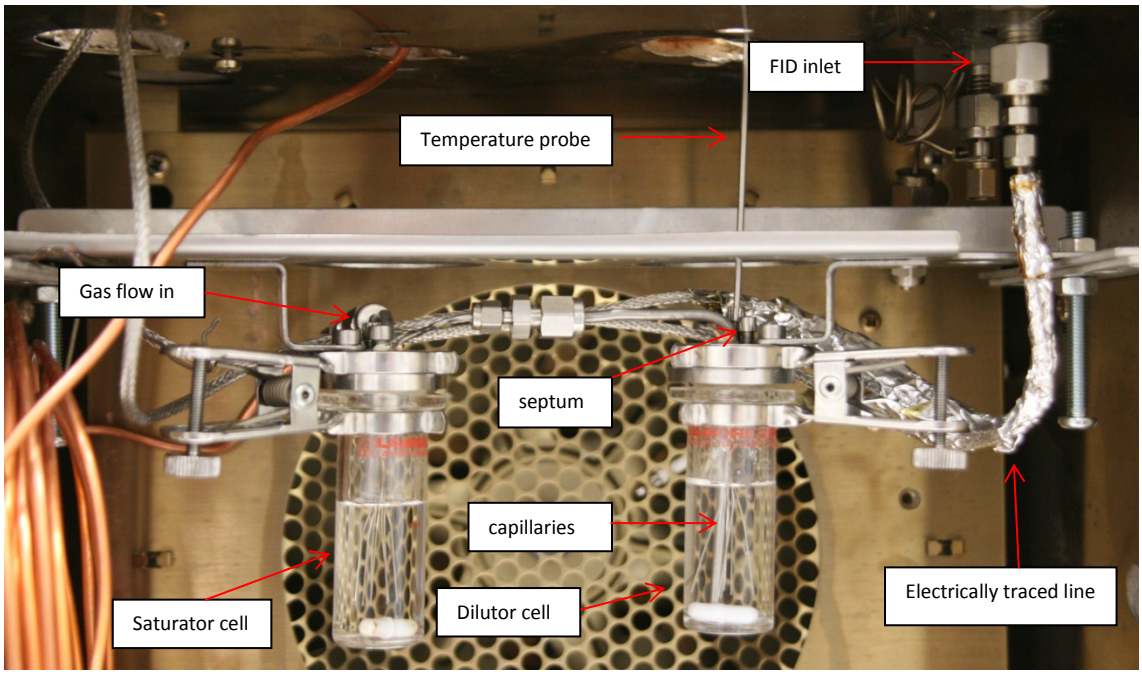

Figure 10 Inert gas stripping equipment

The level of the liquid also plays an important role in a good experiment. It must be made sure that the level of the liquid is not too high to carry the droplet into the gas exit during an experiment. The GC is turned on and flow of Hydrogen and Air is also turned on. The temperature of the detector is set to 275°C, once it is around 50°C it is possible to ignite the flame with a torch. It was observed during the experiments that the ignition does not take place if the dilutor is not attached. One possible reason of this is that other end of the FID being open; this caused disproportionate flow of the ignition gases to the detector which did not allow the flame to be ignited. The temperature of the experiment is set from the interface of the GC and enough time is given so that the temperature of the cell is same as in the oven. The flow of the inert gas is started when the temperature inside the dilutor cell has reached equilibrium. As soon as the flow is started the concentration of the solute in the vapor phase increases and after reaching equilibrium the solute concentration decays exponentially. This concentration change is recorded via Lab View data acquisition software. Along with the FID readings the temperatures are

also recorded and there is also possibility of recording the flow rate of the inert gas. The experiment is stopped when the concentration of the solute in the gas leaving the cell reaches the baseline signal but it is not compulsory.

4. Techniques for solute introduction

During initial tests different solute introduction techniques were tried. All these techniques have their areas of applicability.

1. Vapor Injection
2. Liquid Injection
3. Premixed Solution

Owing to the different nature of solute, different techniques could be applied. Some solutes tend to dissolve quickly in the solvent and other needs vigorous mixing beforehand. The solubility of the solute in the solvent decides which technique is best suited.

4.1. Vapor injection

In this technique the vapor is drawn with a gas syringe from the vapor phase of the vial that contains the pure solute and is injected into the dilutor cell via a septum. The vapors are injected at the height just above the magnetic stirrer to provide maximum path length to the solute gas to achieve efficient mass transfer. When the vapor is injected the first few bubbles arriving in the vapor phase of the cell are not in phase equilibrium with the liquid because they have not completely interacted with the solvent, however with the continuous mixing the equilibrium is achieved quite rapidly and then the elution takes place. It is observed that vapor injections are not suitable for compounds that are a little soluble in water because the solute does not dissolve in solvent and is rapidly eluted out without achieving equilibrium. The elution in this case is not depicting the gas stripping rather it is the solute gas itself leaving the cell without achieving equilibrium. It must be noted that vapor injections must be made very slowly

so that the pressure inside the cell remains constant and enough time is given to solute bubbles for solvent interaction.

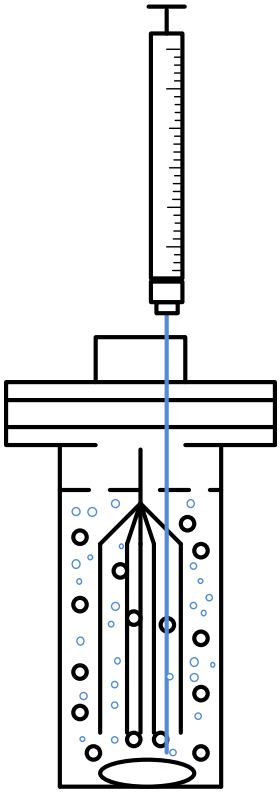

Figure 11 Vapor and liquid injection

It is observed that multiple injections cause the septum to leak and the Teflon piece inside the septum had to be changed. It is proposed that this technique should be tested with very highly soluble compounds so that equilibrium is reached in a short time.

4.2. Liquid injection

In liquid injections an aqueous solution containing the solute is injected to the dilutor cell via a septum with a syringe. This should also be injected at the same height as with the vapors. The liquid dissolution is better than vapor however the solubility of the solute is important. If there is not enough mixing of the solute then equilibrium will not

be reached. Care must be taken that the amount of the liquid is small enough to depict the infinite dilution. The amount of liquid added to the solvent must be recorded and later used in the calculation because it changes the vapor phase volume inside the cell. It was observed during the course of the experiment that if pure solute injection is made then the peak of the solute loading overshoots and then range of the signal must be changed to visualize the elution on the screen. In case of pure liquid injection the amount must be so small that the mole fraction of the solute remains in the infinite dilution range. Liquid injection usually works better with moderately or highly soluble compounds.

4.3. Premixed Solution

Among these techniques, the most reliable is the premixed solution technique for less volatile solutes. In this technique solution of infinite dilution is made in a large quantity for several experiments. The solution is stirred overnight to achieve good mixing, though for compounds with high solubility the mixing time might be shorter. The dilutor cell is now filled with the premixed solution and after weighing it is clipped to the assembly. The experiment is not started until dilutor cell has reached the temperature of the oven. Once the temperature has achieved equilibrium the inert gas flow is started. Premixed solution technique generally works for every type of compound because proper mixing of the solute is achieved. This technique is also advisable because several experiments can be done with the same solution which is prepared beforehand.

5. Elution comparison

Elution curves are recorded with different solution introduction techniques. It is already mentioned that vapor and liquid injections although produce very quick results but are not suitable for every compound type. Hydrophobic compounds must not be tested with these techniques and their solutions must be made prior to the experiment so that enough mixing time is given. In case when efficient mass transfer is not achieved between the gas leaving the cell and the liquid inside the cell then the gas will not be saturated with the solute resulting in lower value of activity coefficient than the original one. A comparison of the elution with different solution preparation techniques is given in figure 12. No difference was observed between vapor and liquid elution behavior.

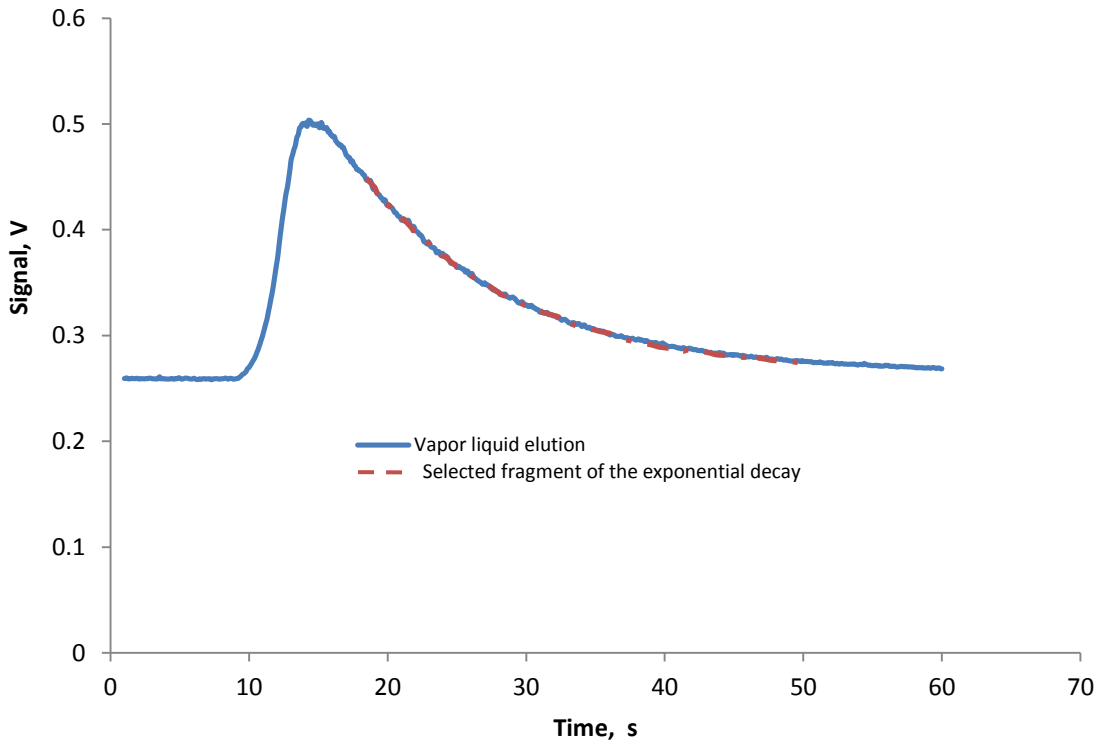

Figure 12 Elution for Vapor and Liquid injections

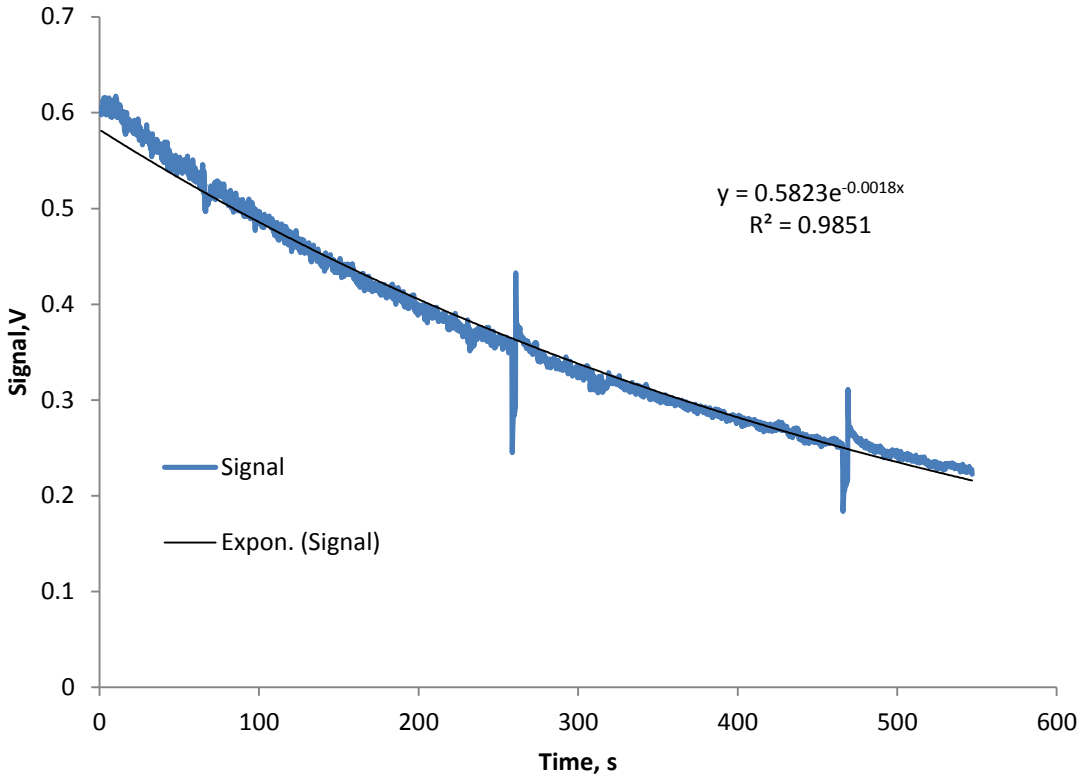

Figure 13 Elution for premixed solutions

It is evident from Fig. 12 that when the solute is introduced the signal reaches to a maximum before it starts to decay exponentially, this maximum is reached very quickly after solute injection but for the purpose of analysis the exponential decay part (visible in red dashed line) of the curve which is in thermodynamic equilibrium is taken into account. The fluctuations appearing in fig.13 could be an outcome of various things including the electric signal disturbance, entrainment, leakages, coalescence of the small bubble or disturbances in the flow rate of the inert gas but it is more probable that they could be a result of electrical signal disturbances or entrainment. The points very close to baseline are neglected due to high noise. The noise in the baseline can be attributed to the temperature non-uniformity of the dilutor cell further investigation is however necessary. It is important to check the baseline before every experiment because the

baseline is a function of temperature and flow rate and the room temperature may also influence the baseline.

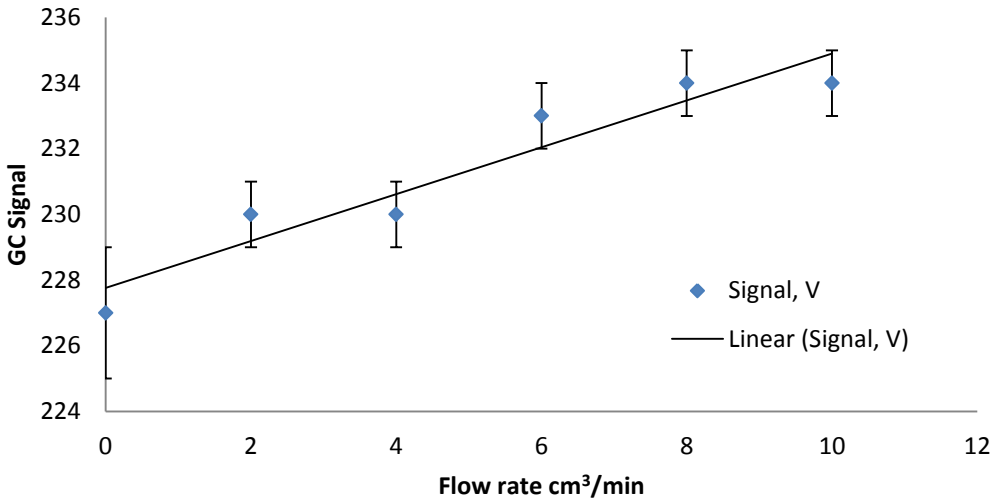

Figure 14 Effect of Flow rate on the baseline

For premixed solution technique the elution is presented in Fig. 13. The elution is recorded once the signal has reached its maximum and it can be seen that it takes a little bit longer depending on the solubility and temperature but this technique is more reliable and ensures that the solute is completely mixed with the solvent. The exponential fit of the curve determines the accuracy of measurement. In some cases the elution curve does not fit to the exponential trend line and this may be because the gas leaving the vapor phase is not in complete equilibrium with the liquid in the cell. It was observed that the fluctuations in the curve increase with the decrease in the flow rate of the inert gas because at slower flow rates the inherent electrical noise is much prominent. It is explained in the later section how flow rate affects the equilibrium of the cell.

6. Results and discussion

The aim of the thesis was to build the inert gas stripping equipment for the measurement of activity coefficient at infinite dilution for compounds present in bio-oil. In this study the activity coefficient at infinite dilution values for two bio-oil compounds (for which literature values are not available) and two reference compounds are reported. The reference compounds used for the validation of the technique are Toluene and n-Butanol. To exploit the range of valid operation with the present system, a parametric approach was followed. Different flow rates and temperatures were tested to inspect the limitations of the current equipment and with these measurements it is deemed to extend the valid operation range of the equipment.

The main difference between this and other equipment used elsewhere (Brockbank et al., 2013; Haimi et al., 2006; Krummen et al., 2000) is that this is capable of recording a continuous change in concentration of solute in the vapor phase of the dilutor cell. Earlier versions of IGS utilized gas sampling valves coupled with GC which draw vapor samples periodically. This difference of data logging made it possible to perform the experiment very fast. Since there is a possibility of continuous data recording, the vapor/liquid solute injection in the dilutor is also easy which makes the experiment really quick especially for checking the repeatability.

6.1. Reference compounds (Toluene and n-Butanol)

In order to validate the dilutor, two reference compounds i.e. Toluene and n-Butanol were used. The reason for their selection was the availability of literature data. The other reason for their selection was a huge difference of their γ^{∞} values (Toluene ~ 9000 and 1-Butanol ~ 45-50 at 298 K) which allows the equipment to be used comfortably for components between these values.

The infinite dilution activity coefficient for Toluene was measured with all different solution preparation techniques but best results were obtained with premixed solution technique. An infinitely dilute aqueous solution of Toluene was made and it was kept well closed under constant stirring for 3 to 4 days before analysis.

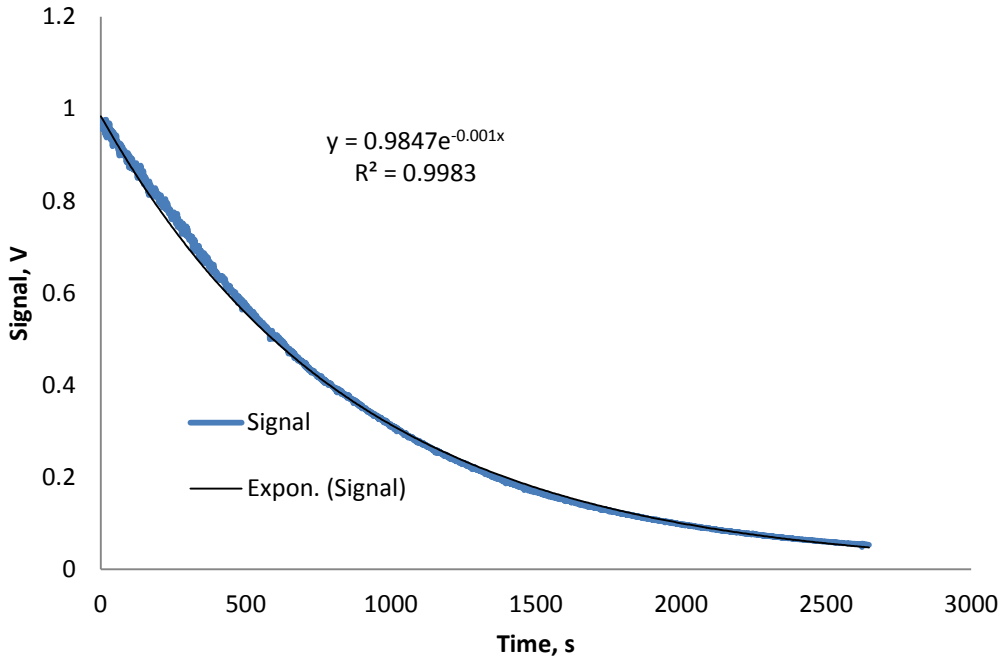

Figure 15 Stripping profile of Toluene at 298 K in water (Premixed Solution)

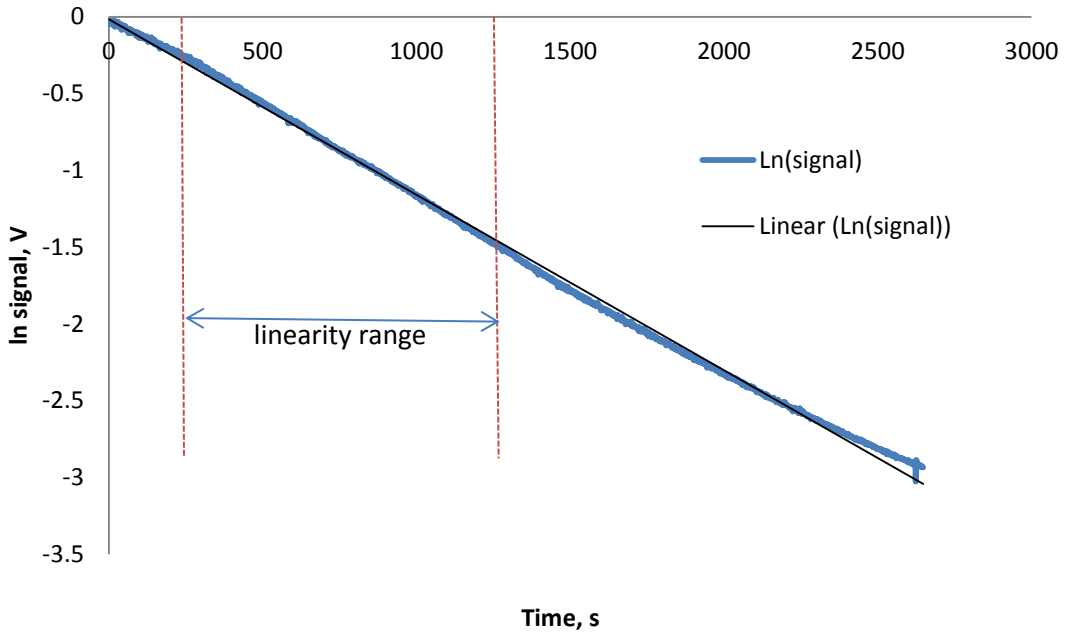

Figure 16 Natural log plot of the stripping profile

Fig.15 illustrates the stripping profile for Toluene at 298 K; It can be seen from the figure that the stripping profile has fluctuations which can more clearly seen if the scale of the figure is magnified. There could be three possible reasons for the fluctuation observed. 1. Entrainment. 2. Condensation. 3. Leakage. We have investigated the possible reasons for this fluctuation. Apparently there is no leakage or condensation in the line. The leakage was tested by a leak detector and since the gas delivery tube is heated by an electrical tracing we assume that there is no condensation of liquid however there could be possibilities of entrainment which can be rectified further by improving the geometry of the cells. The results obtained for Toluene and 1-Butanol at different temperatures and flow rates are tabulated in table 3.

Table 3 Results for the reference systems

Compound	Temp (K)	Flow rate (cm^3/min)	Experimental γ^{∞} value	UNIFAC $\gamma\infty$ estimation value	Lit γ^{∞} value	Lit γ^{∞} value reference
Toluene	**298.15**	4.4	8086	12100	8970	Haimi et al., 2006
	298.15	4.4	7510			
	303.15	4.4	7350	11300	-	-
	303.15	4.4	7290			
	303.15	4.4	7018			
	308.15	4.4	6880	10600	8810	Brockbank et al., 2013
	308.15	4.4	7250			
	313.15	4.4	6450	9920	3249±38	Zhang 1995
1-Butanol	**303.15**	4.4	38	52	51	Whitehead and Sandler, 1999
	313.15	4.4	35	50	49	M.T. Hofstee (European Federation of Chemical Engineering, 1960)

The literature values for the γ^{∞} vary a lot at the same temperature and it is also dependent on the technique used for evaluation. Some literature values for activity coefficient at infinite dilution are calculated from solubility. The inverse of solubility is estimated to be the activity coefficient at infinite dilution, the details of this method is given in the later section. The solubility values vary from each other to a great extent and for components whose γ^{∞} value are high the literature values based on solubility are very different. For instance based on the solubility values the γ^{∞} value for Toluene at 303 K range between 3956 (Salem, 1979) and 17068 (Fuoss, 1943). Activity coefficient based on solubility is not a good measure when the solubility is high. The inverse solubility method for calculation activity coefficient at infinite dilution works when the value of activity coefficient is well above 1000 and in the case of n-Butanol ($\gamma^{\infty} \sim 50$) the calculation of γ^{∞} based on solubility is not correct.

6.2. Bio-oil compounds

6.2.1. Valeraldehyde (Pentanal)

The reason for the selection of Pentanal is already described earlier. Although we have only one literature value available for the activity coefficient at infinite dilution for Pentanal, we were able to compare our values to it. The results seem to be close to the literature values.

Table 4 Results for Valeraldehyde

Compound	Temp (K)	Flow rate (cm^3/min)	Experimental γ^{∞} value	Lit γ^{∞} value	Lit γ^{∞} value (reference)
Valeraldehyde	298.15	-	-	220.2	Kojima et al., 1997
	303.15	4.4	215	-	
	308.15	4.4	223		

Activity coefficients at infinite dilution were determined for 8 different flow rates (as shown in fig. 19) and at the same temperature. Thermodynamically, flow rate of the inert gas must not have any influence on γ^{∞} values provided equilibrium conditions are satisfied consequently there is always an optimum range of flow rate, which comes from the compromise between speed of measurements and perfect equilibrium, results in equilibrium between the gas leaving the cell and the liquid inside the cell. To find the optimum flow rate range for the γ^{∞} determination of Valeraldehyde different flow rates were tested, minor discrepancies were observed among γ^{∞} values and the reported value of γ^{∞} is an averaged value resulting from the flow rates that show minimum deviation. It was observed during the course of this experiment that lower flow rates generally produced more fluctuations than higher flow rates but it can be made sure that the gas leaving the cell has achieved complete mass transfer. Valeraldehyde is very soluble (18 g/dm^3) in water (Samuel et al., 2003) thus it required more time for stripping it than

Toluene. The time for the elution is longer compared to Toluene. This difference in elution behavior can be attributed to the higher solubility of Valeraldehyde and relatively less volatility.

The present dilutor equipment has a limited operational range of temperature. The presence of the heated transfer line inside the GC oven limits its use at higher temperatures, it keeps the temperature of the oven little above the room temperature even when the heating of the oven is not on. There is not a refrigeration unit inside the GC oven which means that it is not possible to lower the temperature of the oven below the room temperature.

6.2.2. n-Hexanoic Acid

Measurements for activity coefficient at infinite dilution were carried out for Hexanoic acid. Several measurements with different flow rates and temperatures were tried but the results were not good. A higher flower rate is needed to reach equilibrium. It is very difficult to strip out n-Hexanoic acid from the solution, with present flow rate possibility, owing to two of its properties. 1. Very low vapor pressure (6.76 Pa at 298K) 2. High aqueous solubility ~ 10 g/dm^3 (Samuel et al., 2003). The elution for n-Hexanoic acid is shown in Fig 17.

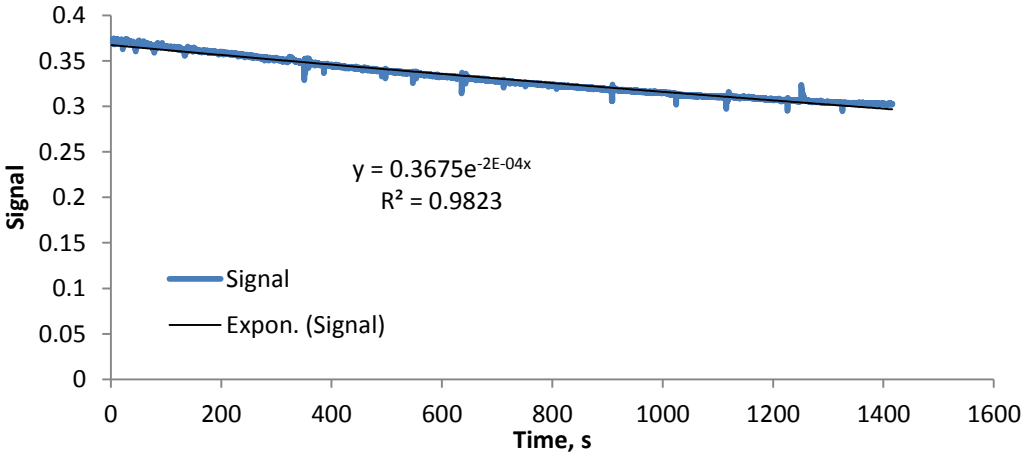

Figure 17 n-Hexanoic acid elution at 298 K

It can be seen that from the figure that the elution is very slow and based on the slope the γ^{∞} value calculated from it is very high (γ^{∞} = 193515) . It is very difficult to get a significant change in the slope for very hydrophilic compounds and the fluctuations are usually higher which makes the activity coefficient determination very inaccurate. Highly soluble compounds such as n-Hexanoic acid needs higher flow rate and longer elution time to strip out of the solvent. The γ^{∞} value from the law of elution is only possible if the solute is volatile enough so that the elution time is not very long. The sufficient variation in the slope is not achievable with compounds with lower volatilities.

Dew point method as pointed out by (Krummen et al., 2000) can be used to determine the activity coefficient at infinite dilution for high boiling solutes.

7. Parametric study

7.1. Effect of temperature

The temperature dependence of the activity coefficient is studied by Tsonopoulos and Prausnitz, 1971. According to their study the variation on activity coefficients for organic compounds with temperature is weak. They have also mentioned that the solubility of organic solids and liquids generally increase with the temperature which has a slight effect on the activity coefficient values; however the established literature values for activity coefficient at infinite dilution at different temperature for different compounds propose that this effect is rather complex especially at infinite dilution. The ample experimental values of γ^{∞} for different compounds are very scattered and it makes it really difficult to predict the temperature dependence of the activity coefficient. As suggested by Hovorka et al., 2002 a simultaneous γ^{∞} determination from partial molar heat capacity or partial molar enthalpy will ensure reliable reasoning for temperature dependence. In their study they examined several moderately hydrophobic solutes and found that all the solutes they examined exhibit a maximum in the range of 273 and 373 K. A very narrow range of temperature was studied in our work and exact temperature dependence over a broad range of temperature cannot be established yet. However the current IGS equipment is capable of reaching the temperature up to 400 K and with few modifications to the auxiliaries of the set up a separate study on the temperature dependency will be done. A comparison of temperature dependence on γ^{∞} is given in the figure 18.

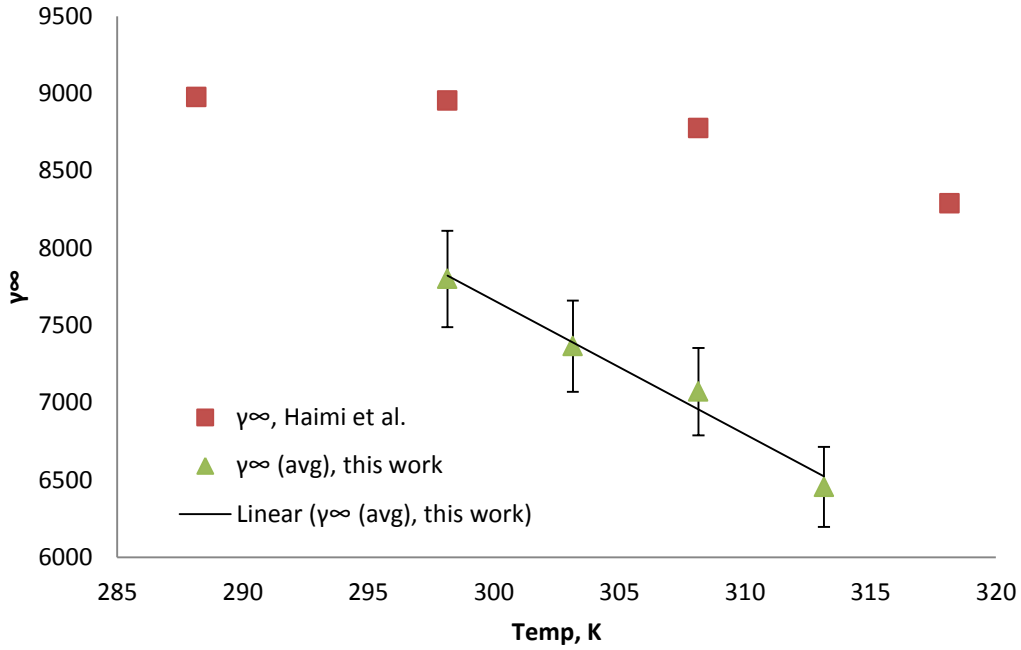

Figure 18 Temperature effect on the infinite dilution activity coefficient for Toluene

In figure 18 above it can be seen that in the temperature range that was investigated, the values for activity coefficient at infinite dilution decrease while temperature increases as evident from two independent studies; however this is only true for the said temperature range and it may not be wise to extrapolate the γ^{∞} values.

7.2. Effect of flow rate

The effect of flow rate is discussed with respect to Valeraldehyde; however it is not a compound specific property and applies generally to every compound. The phase equilibrium implies that flow rate of the carrier gas has no effect on the activity coefficient; however there is always a range of flow rates only which leads to equilibrium. Measured signal values at very small flow rate values tend to have more fluctuations because the signal to noise ratio is very low and the signal value is not

actually measurable. Higher flow rates on the other hand although produces smooth curves but does not necessarily result in equilibrium since the residence time of the bubbles in the cell decreases therefore an optimal flow rate is required for good experiment. A recent article (Brockbank et al., 2013) discusses in more detail about flow rate optimization. It was observed in our experiments that higher flow rates in combination with high stirring speed enhance coalescence of tiny bubbles into big bubbles which prevents from reaching the equilibrium inside vapor phase. The optimum flow rate is different for different compounds however as a general rule of thumb it depends on hydrophobicity of the compound. Highly hydrophobic compounds can equilibrate at higher flow rate and less hydrophobic compounds need longer residence times of the bubbles in the solution for equilibration with the carrier as. This is shown in figure 19 that there is a range of flow rate that produce γ^{∞} values close to each other. The fitness of the stripping curves and their smoothness together determines best range of flow rate that resulted in equilibrium. A poor regression coefficient generally indicates that equilibrium is not reached inside the cell and the carrier gas leaving the cell is not saturated with the solute. It is necessary to find the optimum flow rate for every compound for which it will result in equilibrium, a good practice is to try several flow rates and at least from 3 to 5 different values.

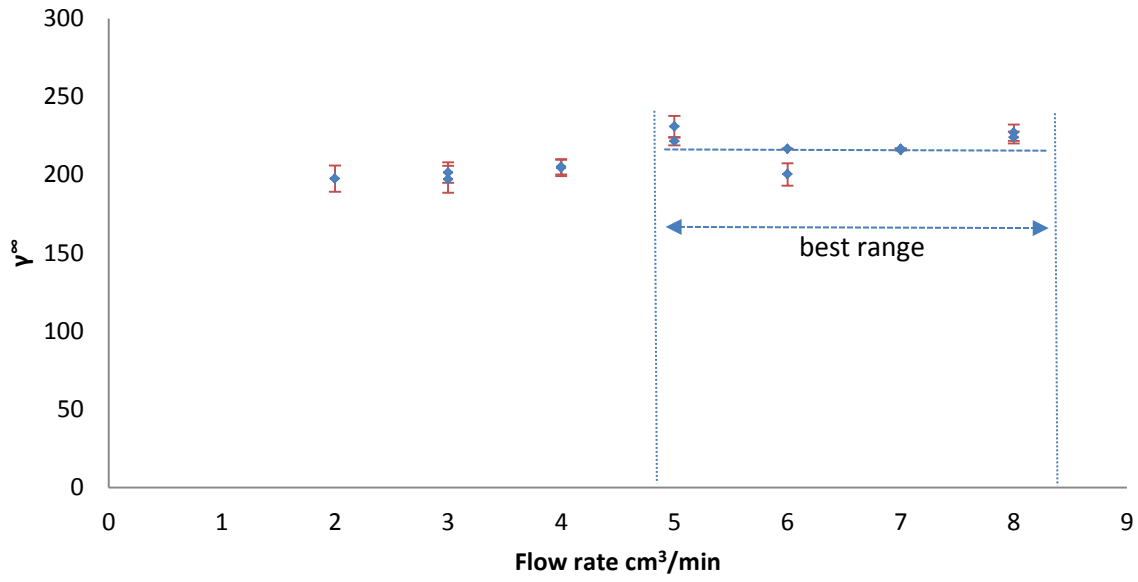

Figure 19 Variation of γ^{∞} with Flow rate, Valeraldehyde at 303.15 K

To study the effect of flow rate on the activity coefficient new system (Valeraldehyde) was analyzed. The purpose was also to acquire confidence in our measurements for a new system. The flow rate was varied from 2 - 10 cm^3/min and it was observed that not much different result was obtained. The activity coefficient value ($\gamma^{\infty} = 215$) obtained at 303.15 K was an averaged value over the optimum flow rate range. As we have explained this earlier as well the solubility of the solute indicates the suitable flow rate, highly soluble compounds need higher inert gas flow rate whereas slightly soluble compounds needs lower inert gas flow rate. Valeraldehyde being highly soluble in water needs higher flow rate for γ^{∞} determination.

7.3. Effect of hydrophobicity

Hydrophobicity of a solute plays an important role in stripping, as a general rule the more hydrophobic the compound is the lesser its association with the solvent will be and faster it will elute from the solution. Hydrophobicity is much confused with volatility even though volatility is an independent property of the compound. The volatility of the solute is also an important parameter to consider but hydrophobicity typically has a much larger contribution in γ^{∞} (Hwang et al., 1992). Hwang et al. have pointed out that stripping is governed by the hydrophobicity of the solute rather than by its pure component vapor pressure. The activity coefficient of hydrophobic organic compounds is high owing to its repellant behavior towards the solvent. The infinite dilution activity coefficient of a compound can be estimated from its solubility as mentioned earlier, this is true because LLE holds that

$$\gamma^s x^s = \gamma' x'$$

Where $\gamma' and\ x'$ are the activity coefficient and mole fraction of the solute in water phase, the solubility of water in the hydrophobic organic phase is very small therefore

γ'can be approximated to unity and the term on the right hand side can also be approximated to unity. The infinite-dilution activity coefficient for sparingly soluble compounds is also close to its activity coefficient at is aqueous solubility, therefore

$\gamma^{\infty} x^{s} \approx 1$

But it should be kept in mind that this is valid for sparingly soluble organic compounds and the results might deviate very much if the solubility is higher.

7.4. Effect of vapor pressure

Pure component volatility although does not have a direct effect on stripping however the mole fraction of solute in the vapor phase is a direct consequence of pure component's vapor pressure at a specific temperature. This effect can be further exploited by analyzing compounds with same solubility and different vapor pressure. Head-space chromatography employs a direct use of vapor pressure or volatility. The mole fraction of solute in the vapor phase is analyzed. The effect of vapor pressure becomes significant with highly volatile solutes at high temperatures. The compounds with high volatility can easily saturate the signal so the working temperature must be checked beforehand. It was analyzed in our measurements that low vapor pressure compounds such as n-Hexanoic acid appear not concentrated enough in the vapor phase. The current technique is not suitable for such compounds.

8. Conclusions

The objective of this research was to design and build a rapid inert gas stripper and to validate it. The design of this equipment is very much based on the design of Professor Richon's (2011) dilutor cell, the only difference being the medium of heating. At current stage the equipment is capable of measuring the activity coefficient at infinite dilution for a large range of components. To validate the range of operability the dilutor was tested with Toluene which is sparingly soluble in water and with n-Butanol which is highly soluble in water.

Flow rate dependence was tested by varying the flow rate of inert gas in an experiment utilizing Valeraldehyde as a solute. The results obtained from varying the flow rate varied between -10 to 16 %. Higher flow rates resulted in better results with more smooth curves. The possible reasons for the discrepancy in the activity coefficient at the lower flow rates could be a result of low signal to noise ratio. We have discussed this earlier that owing to its high solubility, Valeraldehyde requires longer equilibration time and consequently high flow rates are preferred.

Temperature dependence was shown with Toluene and n-Butanol and it was shown that as the temperature increases the activity coefficient at infinite dilution decreases for the range of studied temperatures. The effect of hydrophobicity was also analyzed by comparing the Toluene and n-Butanol and it was observed that hydrophobicity of the solute typically contributes more to the infinite-dilution activity coefficient than the vapor pressure of the solute.

The equipment as validated with two completely different reference systems has been found to allow convenient determination of activity coefficients at infinite dilution for a broad range of compounds.

Inert gas stripping technique is sensitive to various parameters including flow rate, temperature, cell design and vapor phase volume. Careful determination and handling of these parameters will allow improving the accuracy of measurements.

9. Recommendations

The equipment in current stage is capable of measuring activity coefficients at infinite dilution for a large range of components however some recommendations are made to enhance the data quality and improve the equipment operation.

We have observed in literature that most experiments are done at higher flow rates however now with present mass flow controller a maximum flow rate of 10 cm^3/min is achievable. The mass flow controller must be updated to test systems that are highly hydrophobic.

The electrically traced line in the GC oven limits the usage of the oven at higher temperature, since the traced line is heated and there is no refrigeration possibility inside the oven the working temperature cannot be below the room temperature. It might be suitable to keep most of the part of the tube outside the oven to avoid any temperature rise or to reduce the heating medium to a lower power.

The clips that hold the cell with the cap must be robust and leak tight. In present configuration the screws on the clips are changed frequently to prevent any leakages.

The cell design must be optimized to prevent any droplets entrainment and liquid projection on the walls of the vapor space of the cell.

The current data logging system does not allow recording the direct signal; in fact the signal is scaled to a Volt signal ranging from 0 to 1. The data logging of the system must be direct so that there is no need of tuning the signal range.

Multiple liquid and vapor injections cause the septum in the cap to leak and when this is detected in the signal during measurement, the septum is changed. To avoid this frequent leakage due to puncture, the septum material must be changed.

It is recommended that with highly soluble compounds the flow rates must be kept higher so that more bubbles can interact with the solute at the same time. Mass transfer, through stirrer speed adjustment can also be enhanced (stirrer speed increase lead to longer path of bubbles in the liquid phase.)

10. References

Belfer, A. J. Unsteady-state chromatography. *Neftekhimiya* **1972***, 12*, 435-43.

Belfer, A. J.; Locke, D. C. Non-steady-state gas chromatography for activity coefficient measurements. *Anal. Chem.* **1984***, 56*, 2485-2489.

Böhme, A.; Paschke, A.; Vrbka, P.; Dohnal, V.; Schüürmann, G. Determination of Temperature-Dependent Henry's Law Constant of Four Oxygenated Solutes in Water Using Headspace Solid-Phase Microextraction Technique. *J. Chem. Eng. Data* **2008***, 53*, 2873-2877.

Brockbank, S. A.; Russon, J. L.; Giles, N. F.; Rowley, R. L.; Wilding, W. V. Infinite Dilution Activity Coefficients and Henry's Law Constants of Compounds in Water Using the Inert Gas Stripping Method. *Fluid Phase Equilib.* **2013** 45-51.

Brown, R. C. *Thermochemical processing of biomass: conversion into fuels, chemicals and power;* Wiley series in renewable resources. John Wiley & Sons, Ltd: Chichester, West Sussex, United Kingdom, 2011.

Burnett, M. G. Determination of partition coefficients at infinite dilution by the gas chromatographic analysis of the vapor above dilute solutions. *Anal. Chem.* **1963***, 35*, 1567-1570.

Chapoy, A. Phase behaviour in water/hydocarbon mixtures involved in gas production system, *Dissertation,* Ecole des Mines de Paris, 2004.

Eckert, C. A.; Newman, B. A.; Nicolaides, G. L.; Long, T. C. Measurement and application of limiting activity coefficients. *AIChE J.* **1981***, 27*, 33-40.

Eckert, C. A.; Sherman, S. R. Measurement and prediction of limiting activity coefficients. *Fluid Phase Equilib.* **1996***, 116*, 333-342.

European Federation of Chemical Engineering *Proceedings of the International Symposium on Distillation, Brighton, England, 4/5/6 May, 1960: 24th Meeting of the European Federation of Chemical Engineering;* Institution of Chemical Engineers: 1960.

Fuoss, R. M. The System Water—n-Butanol—Toluene at 30° C. *J. Am. Chem. Soc.* **1943***, 65*, 78-81.

Furtado, F. A.; Coelho, G. L. V. Determination of infinite dilution activity coefficients using HS-SPME/GC/FID for hydrocarbons in furfural at temperatures of (298.15, 308.15, and 318.15) K. *J. Chem. Thermodynamics.* **2012***, 49*, 119-127.

Gmehling, J.; Kolbe, B.; Kleiber, M.; Rarey, J. *Chemical Thermodynamics for Process Simulation;* Wiley: 2012.

Haimi, P.; Uusi-Kyyny, P.; Pokki, J.; Aittamaa, J.; Keskinen, K. I. Infinite dilution activity coefficient measurements by inert gas stripping method. *Fluid Phase Equilib.* **2006***, 243*, 126-132.

Hovorka,S.; Dohnal, V.; Roux, A.H.; Roux; D. Determination of temperature dependence of limiting activity coefficients for a group of moderately hydrophobic organic solutes in water. Fluid Phase Equilib. **2002**, 201, 135-164.

Hwang, Y. L.; Olson, J. D.; Keller, G. E. Steam stripping for removal of organic pollutants from water. 2. Vapor-liquid equilibrium data. *Ind. Eng. Chem. Res.* **1992***, 31*, 1759-1768.

I.A. Fowlis, R.P.W. Scott, A vapour dilution system for detector calibration, *Journal of Chromatography A*, **1963**, 11, 1-10

James, A.; Martin, A. Gas-liquid partition chromatography. A technique for the analysis of volatile materials. *Analyst* **1952***, 77*, 915-932.

Kojima, K.; Zhang, S.; Hiaki, T. Measuring methods of infinite dilution activity coefficients and a database for systems including water. *Fluid Phase Equilib.* **1997***, 131*, 145-179.

Krummen, M.; Gruber, D.; Gmehling, J. Measurement of activity coefficients at infinite dilution in solvent mixtures using the dilutor technique. *Ind. Eng. Chem. Res.* **2000***, 39*, 2114-2123.

Krummen, M.; Wasserscheid, P.; Gmehling, J. Measurement of activity coefficients at infinite dilution in ionic liquids using the dilutor technique. *J. Chem. Eng. Data* **2002***, 47*, 1411-1417.

Leroi, J.; Masson, J.; Renon, H.; Fabries, J.; Sannier, H. Accurate measurement of activity coefficients at infinite dilution by inert gas stripping and gas chromatography. *Ind. Eng. Chem. Process Des. Dev.* **1977***, 16*, 139-144.

Li, J.; Carr, P. W. Measurement of water-hexadecane partition coefficients by headspace gas chromatography and calculation of limiting activity coefficients in water. *Anal. Chem.* **1993***, 65*, 1443-1450.

Li, J.; Dallas, A. J.; Eikens, D. I.; Carr, P. W.; Bergmann, D. L.; Hait, M. J.; Eckert, C. A. Measurement of large infinite dilution activity coefficients of nonelectrolytes in water by inert gas stripping and gas chromatography. *Anal. Chem.* **1993***, 65*, 3212-3218.

Li, J.; Paricaud, P. Application of the conductor-like screening models for real solvent and segment activity coefficient for the predictions of partition coefficients and vapor-liquid and liquid-liquid equilibria of Bio-oil-related mixtures. *Energy and Fuels* **2012***, 26*, 3756-3768.

Mokraoui, S.; Coquelet, C.; Valtz, A.; Hegel, P. E.; Richon, D. New solubility data of hydrocarbons in water and modeling concerning vapor-liquid-liquid binary systems. *Ind. Eng. Chem. Res.* **2007***, 46*, 9257-9262.

Oasmaa, A.; Kuoppala, E.; Solantausta, Y. Fast pyrolysis of forestry residue. 2. Physicochemical composition of product liquid. *Energy and Fuels* **2003***, 17*, 433-443.

Oasmaa, A.; Solantausta; Sipilä, K.; Lindfors, C.; Lehto, J.; Jokela, P.; Alin, J. In *In Fast pyrolysis bio-oil: Production, quality, and fuel oil use;* ACS National Meeting Book of Abstracts; 2011.

Perry, R. H.; Green, D. W. *Perry's Chemical Engineers' Handbook, Eighth Edition;* McGraw-Hill Professional Publishing: 2008.

Raal, J. D.; Ramjugernath, D. Rigorous characterization of static and dynamic apparatus for measuring limiting activity coefficients *Fluid Phase Equilib.* **2001***, 187-188*, 473-487.

Raal, J. D.; Mühlbauer, A. L. *Phase Equilibria: Measurement & Computation;* Taylor & Francis Group: 1998.

Reid, R. C.; Prausnitz, J. M.; Poling, B. E. *The properties of gases and liquids;* McGraw-Hill: 1987.

Richon, D. New equipment and new technique for measuring activity coefficients and Henry's constants at infinite dilution. *Rev. Sci. Instrum.* **2011***, 82*.

Richon, D.; Antoine, P.; Renon, H. Infinite dilution activity coefficients of linear and branched alkanes from C1 to C9 in n-hexadecane by inert gas stripping. *Ind. Eng. Chem. Process Des. Dev.* **1980***, 19*, 144-147.

Richon, D.; Sorrentino, F.; Voilley, A. Infinite dilution activity coefficients by inert gas stripping method: Extension to the study of viscous and foaming mixtures. *Ind. Eng. Chem. Process Des. Dev.* **1985***, 24*, 1160-1165.

Zhang, S. J. Postdoctoral research report, *Beijing University of Chemical Technology*, **1995**, 58.

Salem, A. Solubility Data of the System Acetic Acid-Toluene-Water at Different Temperatures. *J. Chem. Eng. Japan* **1979***, 12*, 236-238.

Samuel, H.Y.; He, Y. *Handbook of Aqueous Solubility Data;* Taylor & Francis: 2003.

Sancho, M. F.; Rao, M. A.; Downing, D. L. Infinite dilution activity coefficients of apple juice aroma compounds. *J. Food. Eng.* **1997***, 34*, 145-158.

Smith, J. M.; Van Ness, H. C.; Abbott, M. M. *Introduction to chemical engineering thermodynamics;* McGraw-Hill: 2005.

Snow, N. H.; Slack, G. C. Head-space analysis in modern gas chromatography. *Trends in analytical Chemistry.* **2002***, 21*, 608-617.

Thomas, E. R.; Newman, B. A.; Long, T. C.; Wood, D. A.; Eckert, C. A. Limiting activity coefficients of nonpolar and polar solutes in both volatile and nonvolatile solvents by gas chromatography. *J. Chem. Eng. Data* **1982***, 27*, 399-405.

Thomas, E. R.; Newman, B. A.; Nicolaides, G. L.; Eckert, C. A. Limiting activity coefficients from differential ebulliometry. *J. Chem. Eng. Data* **1982***, 27*, 233-240.

Tsonopoulos, C. An empirical correlation of second virial coefficients. *AIChE J.* **1974***, 20*, 263-272.

Tsonopoulos, C.; Prausnitz , J.M. Activity coefficients of aromatic solutes in dilute aqueous solutions. *Ind. Eng. Chem. Res.* **1971***, 10*, 593-600.

Whitehead, P. G.; Sandler, S. I. Headspace gas chromatography for measurement of infinite dilution activity coefficients of C_4 alcohols in water. *Fluid Phase Equilib.* **1999***, 157*, 111-120.

Wobst, M.; Hradetzky, G.; Bittrich, H. Measurement of activity coefficients in highly dilute solutions. Part II. *Fluid Phase Equilib.* **1992***, 77*, 297-312.

Appendix A (example γ^{∞} calculation)

From the data logger, the signal versus time is plotted.

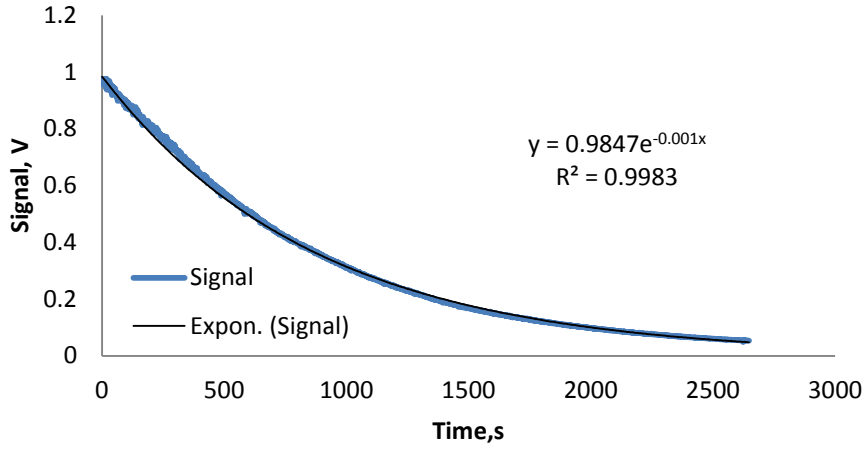

Figure 20 Exponential elution for Toluene at 298 K

The curve in the above figure is an exponential elution/stripping which is evident from the exponential fit. A natural log of this curve is plotted that results in a straight line

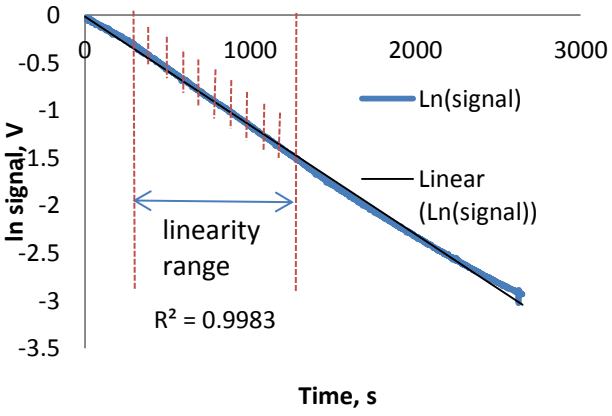

Time, sec	slope	γ^{∞}
100-200	-0.00094	6206
200-300	-0.00101	6694
300-400	-0.00124	8279
400-500	-0.0012	8001
500-600	-0.00125	8398
600-700	-0.00128	8625
700-800	-0.00116	7705
800-900	-0.00115	7691
900-1000	-0.00122	8187
1000-1100	-0.00127	8538
1100-1200	-0.00121	8116
1200-1300	-0.00118	7866

Figure 21 Natural log plot of the stripping profile for Toluene at 298 K and a comparison of slopes at different time intervals in the linearity range.

A linear trend line is fitted to this curve and slope is recorded. It can be seen that the slope only has a small variation in the linear range and for the determination of activity coefficient 100 seconds are enough, making this technique very fast.

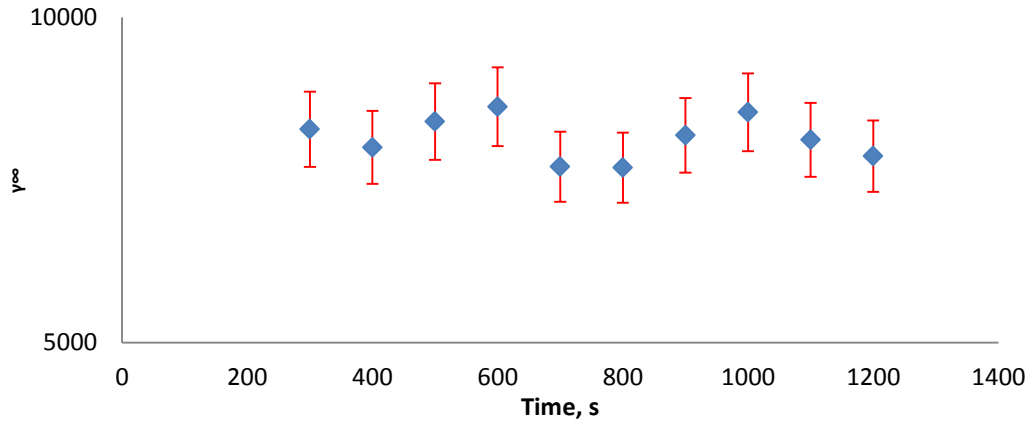

Figure 22 Variation in the γ^{∞} value for Toluene stripping from Water at 298 K

The formula used to calculate the activity coefficient at infinite dilution is

$$\gamma_i^{\infty} = -\frac{n_{solv} RT}{\varphi_i^{sat} P_i^{sat} \left(\frac{F_{in}}{a} + V_g\right)}$$

Sample data:

n_{solv} = number of moles of the solvent = 0.716 moles
R = Universal gas constant = 8314000 Pa cm^3 mol^{-1} K^{-1}
T = Temperature of the dilutor = 298.15 K
φ^{sat} = saturation fugacity coefficient = 0.996
P_i^{sat} = saturation pressure of the solute = 3803.90 Pa
F_{in} = Measured flow rate = 0.075 cm^3/s
V_g = vapor volume of the cell = 4.59 cm^3
a = slope (1/s) = -0.001209577

$$\gamma_i^{\infty} = -\frac{0.716 * 8314000 * 298.15}{0.996 * 3803.9 * \left(\frac{0.075}{-0.001209577} + 4.59\right)} = 8086$$

The solubility of Toluene is the inverse of the activity coefficient at infinite dilution.

$$x_{aq} = {}^{1}/_{\gamma_i^{\infty}} = \frac{1}{8086} = 1.24E - 04$$

Appendix B Fugacity Coefficient

Sample calculation

Critical properties					
	T_c / K	V_c/(cm^3/mol)	p_c / bar	z_c	ω
Water	647.3	57.1	221.2	0.235	0.344
Toluene	591.75	316.0	41.08	0.264	0.264012

Lorentz-Berthelot mixing rules

$T_c mix = (1 - B)\sqrt{Tci * Tcj} = (1 - 0)\sqrt{647.3 * 591.75} = 618.90$ (Binary interaction parameter B set to 0)

$$V_c\ mix = {}^{1}/_{8}\left(\sqrt[3]{Vci} + \sqrt[3]{Vcj}\right)^3 = \frac{1}{8\left(\sqrt[3]{57.1} + \sqrt[3]{316}\right)^3} = 151.50$$

$$Z_c\ mix = \frac{Z_{ci} + Z_{cj}}{2} = \frac{0.235 + 0.264}{2} = 0.2495$$

$$\omega_c\ mix = \frac{\omega ci + \omega cj}{2} = \frac{0.344 + 0.264}{2} = 0.30400$$

$$P_c\ mix = \frac{Z_c R T_c}{V_c} = \frac{0.2495 * 8134000 * 618.90}{151.50} = 84.741$$

Estimation of second virial coefficient, Tsonopoulos Formula

$$B_{virial} = \left(\frac{RT_c}{P_c}\right)\left[B^{(0)} + \omega B^{(1)}\right]$$

Where,

$$B^{(0)} = 0.1445 - \frac{0.33}{T_r} - \frac{0.1385}{T_r^2} - \frac{0.0121}{T_r^3} - \frac{0.000607}{T_r^8}$$

$$B^{(1)} = 0.0637 + \frac{0.331}{T_r^2} - \frac{0.423}{T_r^3} - \frac{0.008}{T_r^8}$$

Where $T_r = T/T_c$.

Virial Coefficients B_{11}= -957.895, B_{12}= -1816.02, B_{22} = -2775.52

Fugacity coefficient (calculated from eq 1-9) = 0.996

Appendix C (Pure component properties)

Pure Component Critical properties and acentric factors (DIPPR 801):

	T_c / K	V_c/(cm^3/mol)	p_c / bar	z_c	ω
Water	647.3	57.1	221.2	0.235	0.344
Valeraldehyde	554	313	35.4	0.256	0.31352
Toluene	591.75	316	41.08	0.264	0.264012
n-Butanol	562.4	274	44.13	0.258	0.59
Hexanoic Acid	660.2	377.2	31.1	0.246	0.733019

Vapor pressure:

DIPPR correlation was used to calculate the vapor pressure its expression is given below:

$$Y = \exp\left[A + \frac{B}{T} + C\ln T + DT^{E}\right]$$

Parameters for DIPPR correlation were taken from DIPPR 801.

	A	B	C	D	E	min temp/K	max temp/K
Water	73.649	-7258.2	-7.3037	4.17E-06	2	273.16	647.096
Valeraldehyde	28.3041	-4657.56	-0.73215	-8.3E-18	6	191.59	566.1
Toluene	76.945	-6729.8	-8.179	5.3E-06	2	178.18	591.75
n-Butanol	106.2948	-9866.35	-11.6553	1.08E-17	6	183.85	563.1
Hexanoic Acid	98.3767	-11394	-10.2239	3.29E-18	6	269.25	660.2

Density of Liquid:

Density of pure liquid was used in volume correction; the correlation is taken from DIPPR. The expression for density calculation is given below:

$$Y = \frac{A}{B^{\left[1+\left(1-T/C\right)^{D}\right]}}$$

Parameters were taken from DIPPR 801.

	Mw g/mol	A	B	C	D	min temp/K	max temp/K
Water	18.015	-13.851	0.64038	-0.00191	1.82E-06	273.16	353.15
Valeraldehyde	86.132	0.8568	0.26811	566.1	0.27354	191.354	566.1
Toluene	92	0.8792	0.27136	591.75	0.29241	178.18	591.75
n-Butanol	74.1216	0.98279	0.2683	563.1	0.25488	183.85	563.1
Hexanoic Acid	116.16	0.62833	0.25598	660.2	0.25304	269.25	660.2

Appendix D- UNIFAC

UNIFAC method

This method is used for predicting the phase equilibria of a system for which no experimental data is available in the literature. The idea behind the method is that compounds can be arranged into structural groups and since the activity coefficient in the mixture is a result of the interaction between these structures, it is possible to predict the behavior of similar structures.

The activity coefficient is a sum of combinatorial and residual term

$$\ln \gamma_i = ln\gamma_i^c + ln\gamma_i^R$$

Where

$$ln\gamma_i^c = ln\frac{\Phi_i}{x_i} + \frac{z}{2} q_i ln\frac{\theta_i}{\Phi_i} + l_i - \frac{\Phi_i}{x_i}\sum_j x_j l_j$$

and,

$$ln\gamma_i^R = q_i\left[1 - ln\left(\sum_j \theta_j \tau_{ji}\right) - \sum_j \frac{\theta_j \tau_{ji}}{\sum_k \theta_k \tau_{kj}}\right]$$

$$l_i = \frac{z}{2}(r_i - q_i) - (r_i - 1)\,, \qquad Z = 10$$

$$\theta_i = \frac{q_i x_i}{\sum_j q_j x_j}, \quad \Phi_i = \frac{r_i x_i}{\sum_j r_j x_j}, \qquad \tau_{ji} = exp\left(-\frac{u_{ji} - u_{ii}}{RT}\right)$$

The residual part is written for solution of groups instead as

Where,

x_i = mole fraction of component i

Θ_i = area fraction

Φ_i = segment fraction/volume fraction

r_i and q_i = volume and surface area parameters

$$ln\gamma_i^R = k\sum_k v_k^{(i)} (\ln \Gamma_k - \ln \Gamma_k^{(i)})$$

Γ_k = group residual activity coefficient

$\Gamma_k^{(i)}$ = reference residual activity coefficient

This group activity coefficient is found from,

$$ln\Gamma_k = Q_k\left[1 - ln\left(\sum_m \theta_m \Psi_{mk}\right) - \sum_m \frac{\theta_m \Psi_{km}}{\sum_n \theta_n \tau_{mn}}\right]$$

where,

$$\theta_m = \frac{Q_m X_m}{\sum_n Q_n x_n}$$

and,

$$\Psi_{mn} = exp\left(-\frac{U_{mn} - U_{nn}}{RT}\right) = \exp\left(-\frac{a_{mn}}{T}\right)$$

U_{mn} = energy interaction parameter between groups m and n

a_{mn}= experimentally determined phase equilibrium parameter

Appendix E (Mass transfer calculation)

When an inert gas is passed through the solution, a thermodynamic equilibrium is reached between the liquid and the carrier gas and the solute is transferred from the solvent to the gas phase. This is achieved in two steps.

1. Mass transfer in the liquid phase
2. Diffusion in the gas phase.

The fractional approach to mass transfer in the liquid phase is given by the equation below

For the derivation of the equations below please see the reference (Richon, D. et al. 1980)

$$\tau_L = 1 - \exp\left[-\left(\frac{3}{R_b}\frac{\rho_L}{M_L}k_L\frac{RT}{P_i^S\gamma^\infty}\frac{h}{\upsilon^\infty}\right)\right]$$

And,

The fractional approach to diffusion in the gas phase is given by

$$\tau_G = 1 - \frac{6}{\pi^2}\sum_{l=1}^{\infty}\frac{1}{l^2}\exp\left[-\frac{D_{ij}^G l^2\pi^2 h}{R_b^2\upsilon^\infty}\right]$$

Where,

ρ_L = density of the solvent (g/cm^3)
k_L = mass transfer coefficient
R = universal gas constant (Pa cm^3 mol^{-1} K^{-1})
T = temperature (K)
h = height of the cell (cm)
R_b = radius of the bubble (cm)
M_L = molar mass of the component (g/mol)
P_i^S = vapor pressure of the component (Pa)
γ^∞ = activity coefficient at infinite dilution
υ^∞ = (7.2 x 10$^{-2}\upsilon_L^{-0.6}D_b^{1.6}$g)^1/1.4 = limiting speed for bubbles in solution (cm/s)
D_{ij}^G = diffusion constant of solute *i* in solvent *j* in gas (cm^2/s)
D_b = diameter of the bubble (cm)
υ_L = kinematic viscosity (cP)
g = gravitational constant (cm/s^2)
τ_L= fractional approach to mass transfer in the liquid phase only
τ_G= fractional approach to diffusion rate through gas phase

Sample calculation: Toluene at 298K

Data

Parameter	Value	Units
ρ_L	0.996	g/cm^3
k_L	0.3	
R	8314000	Pa cm^3 mol^{-1} K^{-1}
T	298	K
h	0.1-3	cm
R_b	0.5-2	mm
M_L	18	g/mol
P_i^S	3862.98	Pa
γ^∞	7440	
υ^∞	variable	cm/s
D_{ij}^G	0.8	cm^2/s

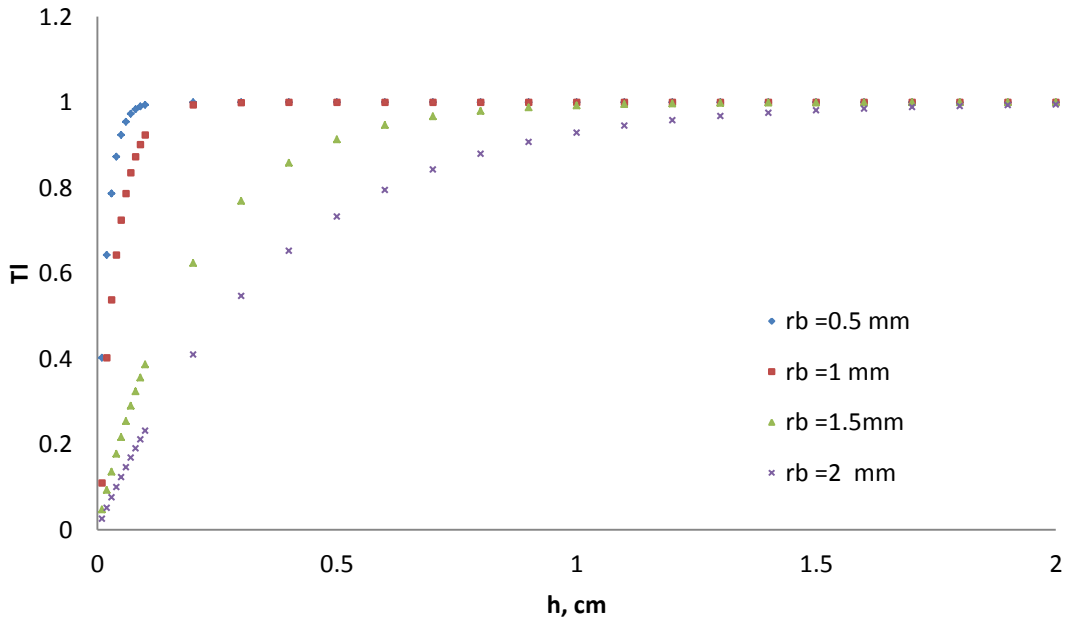

Figure 23 Influence of the bubble diameters on the mass transfer in the liquid phase

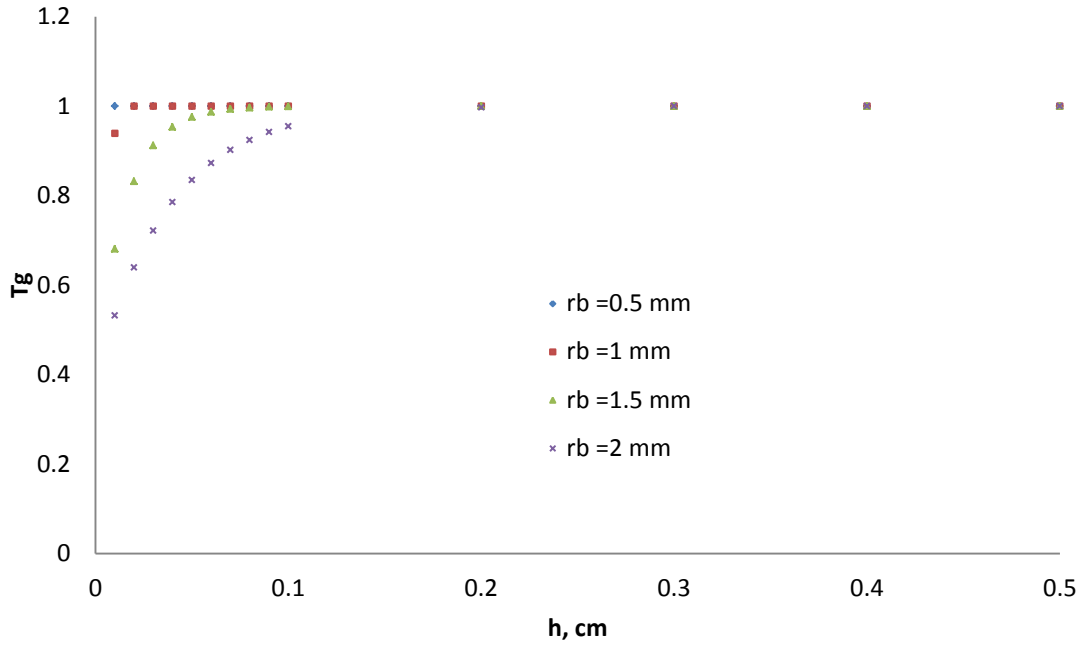

Figure 24 Influence of the bubble diameters on the diffusion rate

Figure 23 illustrates the mass transfer in the liquid phase. The term on the y-axis shows the mass transfer achieved, 1 being the complete mass transfer. On the x-axis is the height of the cell in cm. It can be inferred from the figure that for R_b < 1mm, complete mass transfer is achieved at the height of 1.5 cm. Figure 24 illustrates the diffusion in the gas phase and similar result can be drawn, that for R_b < 1mm the cell with the height of 1 cm is sufficient for complete diffusion. In our case (see fig. 9) the dimensions of the cell are well within the range to achieve efficient mass transfer.

Appendix F (Thermodynamic data availability for bio-oil)

Data base of the Thermodynamic properties available for bio-oil components taken from DDBST. The numbers below represents the data points available in the literature.

ACIDS

	Water	
Name	**VLE (T,P,x,y)**	γ^{∞}
Formic acid	59	3
Acetic acid	154	12
Propionic acid	37	3
Butyric acid	14	n.a.
Hexanoic acid	n.a.	n.a.
Pentanoic acid	1	n.a.
Benzoic acid	2	n.a.
Glycolic acid	1	n.a.

ALCOHOLS

	Water	
Name	**VLE (T,P,x,y)**	γ^{∞}
1,2-Ethanediol	45	10
Ethanol	280	64
Methanol	207	77

GUAIACOLS

	Water	
Name	**VLE (T,P,x,y)**	γ^{∞}
2-Methoxyphenol	5	n.a.
Eugenol	n.a.	3
(cis/trans)-Isoeugenol	n.a.	n.a.
2-Methoxy-4-methylphenol	n.a.	n.a.
Dihydroeugenol	n.a.	n.a.
4'-Hydroxy-3'-methoxyacetophenone	n.a.	n.a.

ALDEHYDES

	Water	
Name	**VLE (T,P,x,y)**	**γ^{∞}**
Acetaldehyde	35	18
Formaldehyde	83	1
Acrolein	10	3
Crotonaldehyde	6	1
Valeraldehyde	1	2
Glyoxal	n.a.	n.a.
trans-2-Methyl-2-buteneal	n.a.	n.a.

FURANS

	Water	
Name	**VLE (T,P,x,y)**	**γ^{∞}**
Furfural	30	2
2-Methylfuran	2	2
Furan	n.a.	n.a.
Crotonolactone	n.a.	n.a.
5-Hydroxymethylfurfural	1	n.a.

PHENOLS

	Water	
Name	**VLE (T,P,x,y)**	**γ^{∞}**
3-Methylphenol	8	6
2-Methylphenol	7	6
4-Methylphenol	1	6
Phenol	47	23
2,3-Dimethylphenol	n.a.	4
2,4-Xylenol	n.a.	6
2,6-Dimethylphenol	n.a.	4
3,5-Dimethylphenol	n.a.	4
2,5-Dimethylphenol	n.a.	4
2-Ethylphenol	n.a.	n.a.
1,4-Dihydroxybenzene	1	n.a.
2,4,6-Trimethylphenol	n.a.	1

Appendix G (Flow meter calibration)

Set point (cm^3/min)	Soap flow meter, measured (cm^3/min)
2	1.82
3	2.71
4	3.63
5	4.44
6	5.38
7	6.31
8	7.14
9	7.94
10	8.88

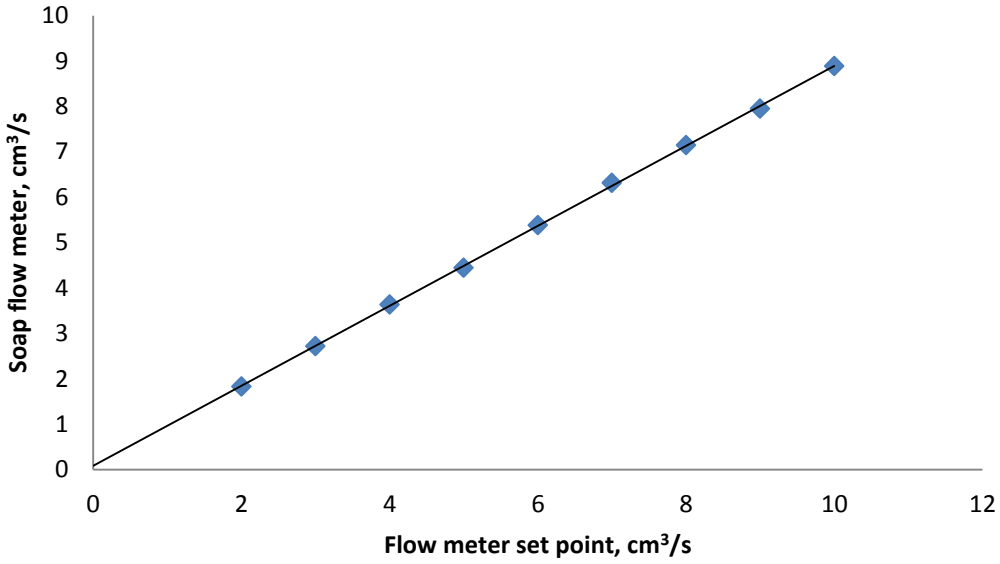

Figure 25 Flow meter calibration